https://doi.org/10.5194/hess-2022-110
Preprint. Discussion started: 25 April 2022

Hydrology and Earth System Sciences
Discussions

Towards a hydrogeomorphological understanding of proglacial catchments : review of current knowledge and assessment of groundwater storage and release in an Alpine catchment

Tom Müller[1,2], Stuart N. Lane[1], and Bettina Schaefli[1,2,3]

[1]Institute of Earth Surface Dynamics, Lausanne, University of Lausanne, Switzerland
[2]Institute of Geography (GIUB), University of Bern, 3012 Bern, Switzerland
[3]Oeschger Centre for Climate Change Research (OCCR), University of Bern, 3012 Bern, Switzerland

Correspondence: Tom Müller (tom.muller.1@unil.ch)

Abstract. Proglacial margins form when glaciers retreat, and create zones with distinctive ecological, geomorphological and hydrological properties in Alpine environments. There is extensive literature on geomorphology and sediment transport in such areas as well as surface and glacial hydrology; but there is much less research into the specific hydrological behavior of the landforms that develop after glacier retreat in and close to proglacial margins. Recent reviews have highlighted the presence of groundwater stores even in such steep, rapidly draining environments. ~~It remains however largely unclear where groundwater recharge and storage occurs and the limited studies of the hydrological functioning of specific landforms has not been put into the perspective of the catchment scale storage discharge behavior driven by proglacial margins~~. Here, we provide a detailed literature review of the geomorphological structure of proglacial landforms in the context of their hydrological processes, as well as a summary of the timescale of their hydrological response. We then propose a recession-analysis based framework to understand how different landforms contribute to catchment-scale discharge. We applied the proposed methods to the case of a Swiss proglacial alpine margin and summarize the insights that follow from a complete perceptual model of how ~~such a~~ proglacial catchments work~~s~~. We identify the relative groundwater storage volumes of different superficial landforms and show how steep zones only store water on the timescale of days, while flatter areas maintain baseflow in the order of several weeks. We show that those geomorphological landforms themselves fail to explain the catchment-scale recession analyses and discuss the presence of an unidentified storage compartment of the order of 40 mm which releases water during the cold months, which we propose to attribute to deeper bedrock flowpaths. Finally, the key insights on the interplay of different landforms as well as the analysis framework is readily transferable to other similar proglacial margins and should contribute to a better understanding of the future hydrogeological behavior of such catchments.

Keywords. glacier forefield, hydrology, groundwater storage, recession analysis, review, Alps, Switzerland

1 Introduction

Glaciated catchments are highly dynamic systems. They are shaped by complex physical, chemical and biological interactions at temporal scales ranging from minutes to decades; and at spatial scales ranging from local processes in the glacier ice to

https://doi.org/10.5194/hess-2022-110
Preprint. Discussion started: 25 April 2022


Hydrology and Earth System Sciences
Discussions

regional effects transmitted via the glacier forefield to downstream regions (Miller and Lane, 2018; Carrivick and Heckmann, 2017). In such environments, where nutrients and energy are limited and climate variations are large, glaciers provide water (Huss et al., 2017), sediments (Hallet et al., 1996) and organic carbon (Brighenti et al., 2019b) to downstream areas, which sustain a high specific biodiversity ~~composed of non-competitive, endemic species~~ (Milner et al., 2009). At the regional scale, glaciers provide a number of ecological services essential for human society, such as water supply for drinking water purposes and irrigation, hydropower or cultural services (Beniston et al., 2018; Haeberli and Weingartner, 2020). Indeed, about a sixth of the world's population depends on glacier melt or seasonal snow packs for its domestic water use (Barnett et al., 2005), with this dependence showing strong regional differences as a function of precipitation seasonality (Kaser et al., 2010; Viviroli et al., 2007), groundwater interactions (Vincent et al., 2019) and artificial water storage capacities (Christensen and Lettenmaier, 2007).

Water resource availability is undergoing strong seasonal modifications due to climate warming with rapid retreat of glaciers worldwide (Milner et al., 2017). Indeed, Huss et al. (2017) estimated a glacier volume loss between 2010 and 2100 of 84±15% in the European Alps and of 80±10% for the sub-tropical Andes. Peak annual runoff from glacier melt will be reached between 2010 and 2060 across the world (Huss and Hock, 2018) and the subsequent reduction of ice available to melt, together with more liquid precipitation and earlier snowmelt (Lane and Nienow, 2019; Klein et al., 2016) will cause a change of streamflow regimes, with a shift in the magnitude and the timing of high flow to earlier in the snow melt period (Berghuijs et al., 2014; Beniston et al., 2018; Gabbi et al., 2012; Lane and Nienow, 2019). Glacier melt changes will be especially challenging for Central Asia and South America, where the largest reduction of basin-scale runoff (>30%) has been observed (Huss and Hock, 2018) and where rural populations with low adaptation capacity may be severely impacted (Buytaert et al., 2017), a problem that may then extend to growing lowland populations that rely on mountain runoff, notably in Central, South and East Asia (Viviroli et al., 2019).

Whilst multiple discussions of the implications of cryosphere changes (e.g., Beniston et al., 2018; Huss et al., 2017; Immerzeel et al., 2020) have emerged, the role of groundwater is typically neglected in many glacio-hydrological studies in Alpine environments (Vuille et al., 2018). This is surprising given the rapidly growing body of literature on groundwater–snowmelt interactions. e.g. for environments with regular droughts (Fayad et al., 2017; Jefferson et al., 2008). Such studies show that groundwater resources may play an important role in maintaining baseflow and in compensating for limited snow cover during droughts (Van Tiel et al., 2021), especially where glacier cover is small, as also suggested in regional studies in the Andes (Vuille et al., 2018) and in the Himalayas (Andermann et al., 2012; Yao et al., 2021). The implications of rapid glacier retreat for ice melt-groundwater interactions are also largely neglected, an issue that will be amplified as in years with snow drought, reduced snow accumulation causes a more rapid and earlier transition to ice cover, with lower albedo and a more rapid melt. Large areas of previously ice-covered till and bedrock are becoming exposed in proglacial margins, leading to frequent geomorphological changes (Heckmann and Morche, 2019) and the emergence of landforms prone to groundwater storage (Hayashi, 2020).

Reasons that might explain a certain disconnection of glacio-hydrological research in mountain environments from groundwater research include i) a focus upon water storage above ground (in the form of snow and ice); ii) the absence of groundwater-

https://doi.org/10.5194/hess-2022-110
Preprint. Discussion started: 25 April 2022


Hydrology and Earth System Sciences
Discussions

sustained summer low flows in such environments, which typically show a summer high flow; iii) very few studies of the hydrology of glaciated catchments through the winter when the ice and sow melt contribution is much less important than in summer iv) the wide-spread use of conceptual hydrological models with highly simplified representations of groundwater (e.g. Schaefli et al., 2014; Huss et al., 2008) and iv) the historical representation of glaciers as overlying impervious bedrock.

The hydrological response of a proglacial margin in terms of water partitioning, storage and release (Wagener et al., 2007) depends strongly on the sedimentological structure of landforms and on their rapid modification occurring with glacier retreat. Understanding landform formation is thus essential; in the following, we first review key geomorphological processes, followed by what is known about the hydrological functioning of proglacial landforms.

1.1 Geomorphology of proglacial landforms

Current proglacial margins are usually defined based on the Little Ice Age (1850) glacier extent (Heckmann et al., 2019). The geomorphological processes occurring here (also called "paraglacial" processes) can be separated into (i) gravitational processes linked to glacial debuttressing and rock slope failure (Grämiger et al., 2017), debris flow (Ballantyne, 2002) and freeze-thaw cycles (Haeberli et al., 2006) (ii) glaciofluvial processes linked to river erosion, transport and deposition of sediments and neighboring landforms (Lane et al., 1996; Maizels, 2002); and (iii) processes associated with relict ice and its melt-out (Evans et al., 2006). Landform assemblages in proglacial margins are complex and have been created by the history of glacial advances and retreats and complex paraglacial reworking processes. A typical landform assemblage is proposed in Fig. 1.

In the following, we briefly discuss the origin of these landforms.

1.1.1 Sediments, lateral moraine deposits, debris cones, alluvial fans and talus slopes

Due to high glacial erosion rates, on the order of 0.1 to 10 mm yr-1, on crystalline bedrock (Hallet et al., 1996; Guillon et al., 2015) and the efficiency of subglacial channeled streams to transport sediments, glaciogenic sediment supply (also called "till") is the main sediment source to the proglacial area (Guillon et al., 2015). The majority of subglacial sediments are produced at the bedrock-ice interface due to glacier erosion through glacial abrasion, glacial plucking or quarrying or meltwater erosion (Bennett, 2009) and are then deposited or transported by a number of mechanisms including basal ice regelation, upward faulting and folding (Alley et al., 1997) or subglacial streams (Swift et al., 2005). Regardless of their degree of consolidation, most glacial tills are classified as diamicton, refering to a material composed of non-sorted sediments where particle size ranges from very fine clays to gravel (Evans et al., 2006). The basal debris layer that forms under glaciers is called hereafter traction till and is affected by high ice pressure and shear stress, leading to a more compacted and more impervious material. Traction till can be distinguished from subglacial melt-out till, which refers to englacial sediments released by basal melting deposited without deformation (Evans et al., 2006). Such melt-out till has a similar particle distribution but is less packed and contains fewer fines.

Lateral moraine deposits form by three main processes: i) subglacial and supraglacial sediment deposition during glacial retreat; ii) gravity and fluvial flow leading to reworking in steep parts (>30°(Dusik et al., 2019)) and creation of gullies

https://doi.org/10.5194/hess-2022-110
Preprint. Discussion started: 25 April 2022

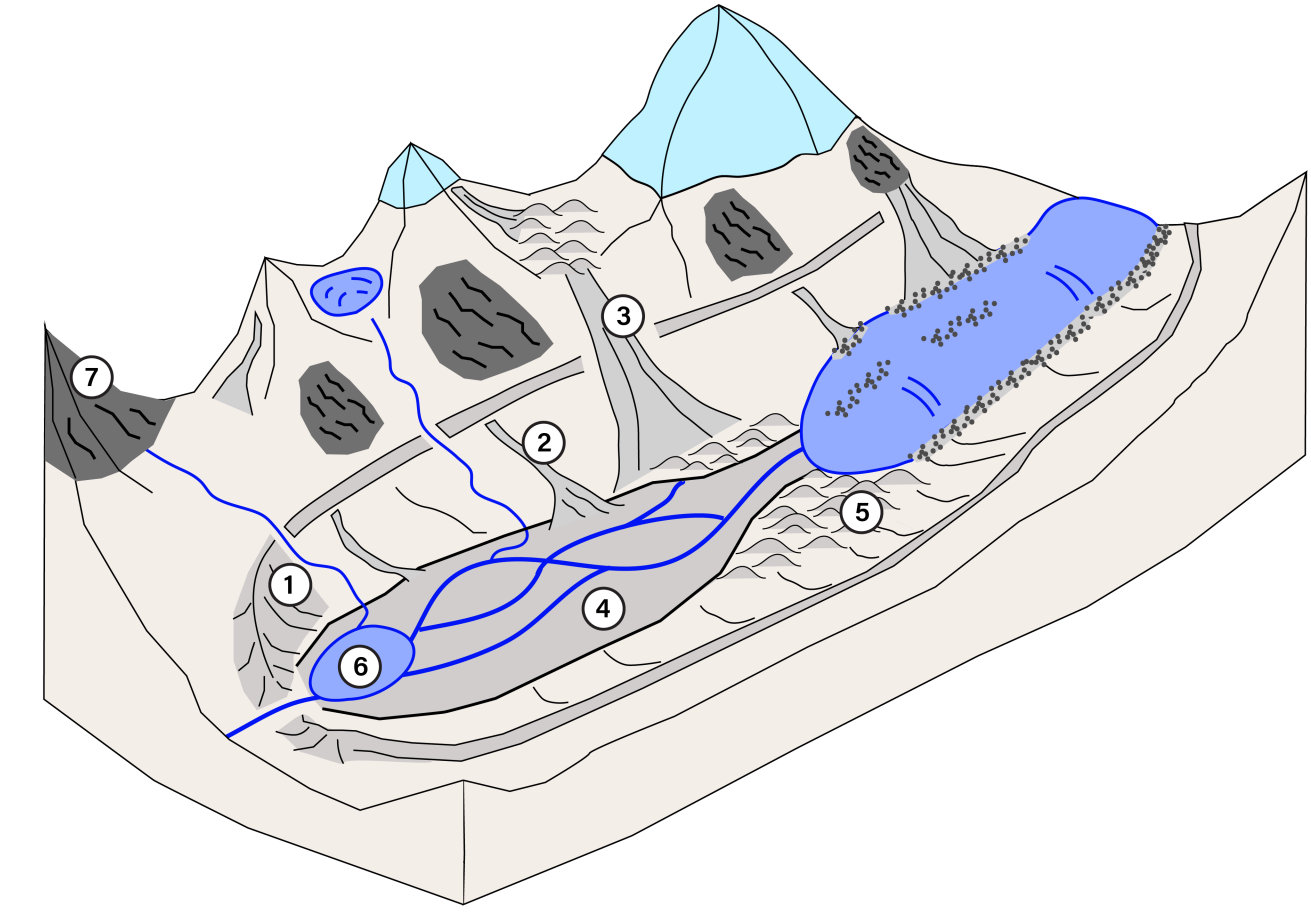

Figure 1. General overview of geomorphological landforms typical of proglacial zones. 1) Lateral moraine; 2) Debris cone; 3) Talus slope; 4) Outwash plain; 5) Glacial deposit (till) ; 6) Proglacial lake ; 7) Apparent bedrock (figure inspired from Temme (2019))

(Mancini and Lane, 2020) and iii) glacier readvance that erodes earlier deposits and "plasters" the remaining deposits (Lukas and Sass, 2011; Lukas et al., 2012). Lateral moraines are mainly composed of a non-sorted mix of fine to coarse materials and potentially have a more consolidated till. The paraglacial reworking of the moraine leads to sediment accumulation on previous glacial deposits in the lower part of the lateral moraine (Mancini and Lane, 2020). Such debris cones are composed of poorly sorted sediments and have a typical slope angle of 12-25°(Ballantyne, 2002). Their sedimentological signature is similar to the underlying moraine deposits, with the exception of showing more slope-parallel stratification and lenses of silty-sand linked to alluvial deposition (Curry and Ballantyne, 1999). Alluvial fans are distinguished from debris flow-based fans by their gentler slope (<15°) and are usually composed of sediments from both debris flow and fluvial deposition. Compared to debris-cones, the debris of talus slopes originates from rock slope failures and is not necessarily linked to glaciogenic materials. Depending on their extent, these landforms may flow above or may be mixed with lateral moraine deposits or glaciofluvial sediments.

https://doi.org/10.5194/hess-2022-110
Preprint. Discussion started: 25 April 2022


Hydrology and Earth System Sciences
Discussions

Talus slope debris is coarser than morainic material, more angular and usually less compact. It accumulates downslope in the form of stratified layers. In its lower part, talus slope debris usually sits on pre-existing soils or on moraine formations, in its upper part, it usually sits directly on the bedrock (Sass, 2006, 2007).

In the flatter valley bottom, glaciers deliver substantial amounts of sediment. Glacier retreat commonly leads to deposits that comprise tills stacked on top of each other. Traction till usually represents the lowest layer and is the most consolidated and fine material (Hammer and Smith, 1983; Eyles et al., 1983). Subglacial melt-out till may be released near the glacier front (Hart, 1998), leading to a less compacted stratified diamicton (Eyles et al., 1983). If the englacial debris load is important, supraglacial accumulation can occur at the glacier front, leading to hummocky moraines which usually trap and isolate large blocks of ice (see Permafrost, rock glaciers and ice-cored moraines). The thickness and ratio of both traction and melt-out till depends on the characteristics of each glacier and can vary substantially. Generally, in Alpine environments, basal traction till was reported to be very thin and rather discontinuous (<1m (Iverson et al., 1994; Brand et al., 1987; Kulessa et al., 2005)), so that a strongly consolidated, low conductive layer does not seem to occur in most moraines (Lukas, 2012). Therefore, glacial till deposits are mostly constituted by a stratified diamicton composed of silt to sandy-gravelly sediments (Rogger et al., 2017) and should be less compacted than lateral moraines due to the absence of a "plastering" mechanism.

1.1.2 Glaciofluvial landforms, the outwash plain, proglacial lakes

Subglacial streams usually come in contact with glacial deposits at the glacier tongue. Due to strong diel streamflow variations and occasional large floods, a strong reworking of the valley floor occurs, with a succession of phases of erosion and aggradation and a usual eluviation of fines (Marren, 2005). Where the valley slope is low, stream power decreases and sediment sorting occurs (Miall, 1977), with coarser sediments deposited in the proximal region and finer sandy material deposited further downstream (Zielinski and Van Loon, 2003). If the accommodation space is large, thick deposits of sandy-gravelly material will lead to the creation of bars and of a braided stream network, eventually leading to the creation of so-called glaciofluvial outwash plains (Maizels, 2002), which may play an important role as sediment traps (Baewert and Morche, 2014; Lane et al., 2017). They are composed of heterogeneous layers of non-consolidated silty-sandy and gravely facies (Anderson, 1989; Ballantyne, 2002), and they usually sit on previously deposited reworked glacial till, composed of a finer diamicton layer (Maizels, 2002). The burial of ice blocks is also a common phenomenon, leading to the formation of “kettle holes” (Maizels, 1977).

Proglacial lakes usually form behind a natural barrier which can originate from (i) an overdeepening in the bedrock; ii) a frontal moraine-dam; iii) an ice-dam or iv) a landslide-dam (Otto, 2019). Many small proglacial lakes are ephemeral due to the gradual or sudden rupture of the natural dam, and may cause extreme events such as glacier lake outburst floods (GLOFs) (Nie et al., 2018). They act as a sediment trap for all types of sediments, mainly from fluvial origin through sedimentation of the suspended load, from melt-out of ice blocks or from debris from the valley sides. The most common moraine-dammed lakes are usually composed of glaciofluvial sediments forming annual layers of coarser material (silt/sand) in summer and finer deposits in winter, which can be overlain by more outwash sediments once the lake becomes filled with sediments (Ballantyne, 2002). Due to the fine nature of their sediments, proglacial lake sediments are usually rather unproductive, but may constitute important natural water reservoirs (Parriaux and Nicoud, 1990).

https://doi.org/10.5194/hess-2022-110
Preprint. Discussion started: 25 April 2022

Hydrology and Earth System Sciences
Discussions

1.1.3 Permafrost, rock glaciers and ice-cored moraines

Permafrost is defined as a ground ~~thermal state~~ where temperature is at or below 0°C for a minimum of two years (Haeberli et al., 2006). The frozen material is usually located a few meters below an active-layer of unfrozen sediments and plays an important role in stabilizing slopes and moraines and thus limiting sediment transport. Increased permafrost thawing due to warmer temperature is expected to reduce slope stability, leading to further reworking of hillslopes and hazardous events such as landslides or moraine-dam lakes breaches (Haeberli et al., 2017), and may also be a source of water for high Alpine environments (Gärtner-Roer and Bast, 2019). While permafrost thaw ~~will~~ not directly yield large water volumes (Harrington et al., 2018), permafrost may occupy part of an aquifer, leading to impervious layers, limiting deeper water infiltration and thus aquifer volume. Indeed, Rogger et al. (2017) modelled the future groundwater storage capacity due to the complete removal of permafrost in a small glaciated catchment and calculated a 19% increase of runoff during the autumn recession period.

Rock glaciers are periglacial landforms intrinsic to the presence of permafrost and their future role for providing water supply and chemical compounds has been stressed recently (Brighenti et al., 2019a). Rock glaciers may be classified based on the genetic origin of their ice and debris into two types: i) rock glaciers derived from talus slope processes under permafrost conditions and ii) heavily debris-covered relict glaciers in permafrost free zones. The definition of the latter as rock glaciers is still not clear in the literature. Berthling (2011) addresses this confusion by defining rock glaciers as “the visible expression of cumulative deformation by long-term creep of ice/debris mixtures under permafrost conditions”. Accordingly, degenerating melting debris-covered glaciers are excluded from this definition because of the absence of permafrost conditions. These formations are recognized as ice-cored moraines and have a similar composition to glacial till deposits, usually with a more important depletion of fine materials (Haeberli et al., 2006).

Most rock glaciers are thus slope-derived in permafrost zones and are created by the burial of surface snow and ice by debris from talus slopes. They are composed of a matrix of coarse blocky sediments with a lack of fine materials and a frozen core of fine-grained to larger sediments (Haeberli et al., 2006).

1.2 Hydrological functioning of proglacial margins and landforms

Proglacial margins are characterized by a strong seasonal streamflow regime, with low flow during winter, conditioned by below-zero air temperature and near ubiquitous snow cover. The onset of snow-melt leads to a gradual streamflow increase in spring, with the highest flows and the largest diurnal fluctuations (Lane and Nienow, 2019) occurring after near complete snow disappearance and the development of a strong subglacial channelized stream network (Werder et al., 2013). In autumn, the decreasing air temperature and solar radiation stop ice melt and lead to the onset of snowfall, which explains the return to winter baseflow. The relative contribution of precipitation, snow-melt, ice-melt and groundwater during each season is to date not well understood and greatly depends on the glacier coverage (Van Tiel et al., 2020; Schmieder et al., 2018). Historically, high Alpine catchments were considered as "Teflon basins" where all water inputs are quickly directed into streams (Williams et al., 2015). This vision was supported by a highly simplified representation of the geology of the system : an impervious bedrock with

https://doi.org/10.5194/hess-2022-110
Preprint. Discussion started: 25 April 2022


Hydrology and Earth System Sciences
Discussions

very coarse glacial deposits having little retention capacity. Some studies have tried to address this lack of understanding at the catchment-scale, using end-member mixing model or water balance approaches.

At the catchment-scale, stable isotopes of water have been increasingly used as a conservative tracer to quantify the contribution of different water sources (Beria et al., 2018). They are often combined with other geochemical tracers such as electrical conductivity (EC) or chloride (Crossman et al., 2011) to create three-component mixing models. Based on such models, (Penna et al., 2014) showed a delayed contribution of snowmelt to spring water compared to stream water, and a peak snow contribution of up to 92% during July and August, when most of the snow had disappeared from the catchment. These observations suggest relatively long groundwater recharge times and challenge the "Teflon hypothesis". Groundwater contribution was also shown to contribute significantly to streamflow, from a minimum of 20% during summer for a 25% glaciated catchment and up to 90% in autumn (Engel et al., 2016; Penna et al., 2017). A growing groundwater contribution with distance downstream (decreasing percentage of glacier cover) is also observed in summer, from 20% to 50% for sub-catchments of 25% to 4% glaciated surface (Penna et al., 2017). However, the choice of end-members, as well as the spatial distribution and timing of sampling has resulted in uncertainties in such studies (Schmieder et al., 2018). The use of EC as a tracer of groundwater may be questioned, since groundwater EC, may not be considered homogeneous in groundwater due to preferential flow paths (Zuecco et al., 2019) and does not take into account possible increase due to the re-emergence of surface water due to fast hyporheic exchanges (Kalbus et al., 2006).

Isotope analyses have also been used to assess groundwater travel time distribution using various models (McGuire and McDonnell, 2006), but long continuous time series are needed (Benettin et al., 2017), limiting their feasibility during winter in snow-covered areas. One tentative study (Schmieder et al., 2019) identified a mean response time of 28 days for a small groundwater dynamic storage in a 34% glaciated, crystalline catchment, but there was also much larger "mobile storage" (see Staudinger et al., 2017) with a mean transit time of 9.5 years, indicating both a fast catchment response and a much slower subsurface storage reservoir. Finally, isotope-aided glacio-hydrological models may also provide more reliable estimates of the contribution of different compartments at the catchment-scale (He et al., 2019).

There are also water balance-based approaches for groundwater storage quantification in highly glacierized catchments that try to characterize all incoming (snow melt, precipitation, glacier melt) and outgoing fluxes (streamflow, evapotranspiration, sublimation). Hood and Hayashi (2015) used a dense snow survey to characterize maximal snow depth and density, combined with a snowmelt model and snow transects in a small 4% glaciated catchment and found an early groundwater storage increase of 60-100mm by the end of June, and a gradual storage decrease in August and September that they attributed to drainage of extensive proglacial moraines. Using a similar approach, Cochand et al. (2019) used airborne LIDAR scanning to estimate maximum snow height distribution in a small headwater catchment with two small rock glaciers (1.5% coverage) and showed an early summer snowmelt-related groundwater storage increase of 300±60 mm, attributable to an evaporitic rock layer.

While studies at the catchment-scale provide valuable understanding of the overall hydrological functioning of such proglacial margins (e.g. Hood and Hayashi, 2015; Andermann et al., 2012; Penna et al., 2017; Engel et al., 2016; Cochand et al., 2019; Engel et al., 2019), the internal mechanisms responsible for such behavior remain difficult to identify, making future predictions difficult in such geomorphologically dynamic systems. In particular, as the importance of groundwater in

https://doi.org/10.5194/hess-2022-110
Preprint. Discussion started: 25 April 2022


Hydrology and Earth System Sciences
Discussions

recently deglaciated catchments has been acknowledged in recent review papers (Vincent et al., 2019; Glas et al., 2018), there is a need for a clearer view of the hydrogeological functioning of their landforms, which is discussed hereafter.

There are a few existing studies on the hydrology of outwash plains, which have however mostly been studied in ice-cap glaciers (Ó Dochartaigh et al., 2019; Mackay et al., 2020), where these plains can become very large and are referred to as sandurs (Robinson et al., 2008; Levy et al., 2015; Macdonald et al., 2016). They have been found to be large productive aquifers with important surface-water groundwater interactions, with glacier meltwater contributing to wells up to 500 meters from the stream (Ó Dochartaigh et al., 2019). A few studies in the Alps (Ward et al., 1999; Malard et al., 1999; Crossman et al., 2011), showed that outwash plains behave similarly to larger sandurs, similarly collecting water from multiple sources and maintaining various groundwater-fed river channels in autumn and winter, promoting habitat heterogeneity and high biodiversity. A study in a late Pleistocene glaciofluvial plain also showed its large water storage capacity and a smooth aquifer depletion during a seasonal drought, where it contributed up to 35% of the streamflow of a 194 km^2 catchment while only representing 3% of its surface(Käser and Hunkeler, 2016). Another study of a glacially deposited alluvial system in Canada showed that up to 50% of the river baseflow could originate from an upward groundwater exfiltration in the downstream part of the alluvium deposits (Schilling et al., 2021). However these studies are based on older, larger deposits, while recent proglacial outwash plains emerging after the little ice age are expected to be smaller and store less sediment, making their hydrological significance less clear.

In addition to studies on outwash plains where fluvial reworking is important, there are some specific studies on the groundwater-surface water interactions of glacial till which usually have slightly steeper slopes and are less fluvially reworked. For example, in a catchment in Alaska, 46% of annual streamflow was lost to a till aquifer and was the main contributor for lowland winter streamflow (Liljedahl et al., 2017). Three studies on proglacial moraines in the Swiss Alps (Magnusson et al., 2014; Kobierska et al., 2015a, b) documented an aquifer alimented by the stream and a groundwater table close to the surface ($< 1m$) flowing parallel to the stream. Reporting an aquifer thickness of 10 m and a slow reservoir response time of 29 days, they showed that such an aquifer might provide baseflow during the entire winter season. Apart from these studies of glacial till and outwash plains, there is a series of studies on the hydrological functioning of ice-cored moraines and rock glaciers. Most studies on ice-cored moraines have shown a hydrological response composed of a fast and slow groundwater component that could sustain substantial winter baseflow (Langston et al., 2011). Harrington et al. (2018) published a multi-method analysis of such rock glacier where they showed a 1 to 2m saturated finer basal layer with a response time of 20 days overlain by a coarser layer having a much higher hydraulic conductivity. Large ice blocks and ground ice are also reported but were too sparse to be considered as an aquitard. Winkler et al. (2016) reported similar behavior, but with a lower less conductive layer attributed to traction till.

There is no clear consensus in the literature about the hydrological functioning of talus slopes and on their role for groundwater storage, release and hence baseflow. Clow et al. (2003) showed that talus slopes were composed of a finer, more compacted lower layer and of a coarser upper layer; Clow et al. (2003) furthermore showed an aquifer thickness of a few meters and concluded that talus slopes contributed up to 75% of winter baseflow. Liu et al. (2004) also pointed out the importance of talus slopes, but mainly in conveying snowmelt to downslope parts of the catchment, adding little water to winter baseflow.

https://doi.org/10.5194/hess-2022-110
Preprint. Discussion started: 25 April 2022


Hydrology and Earth System Sciences
Discussions

On the other hand, Muir et al. (2011) reported fast hydraulic conductivity and very little capacity to maintain baseflow for more than a few days (response time of about 1 day) due to the coarse texture of talus slopes. They estimated a very thin saturated layer (<0.03m) at the talus-bedrock interface. Due to the dominance of pre-event water during storms and due to the lack of visible finer sediment layers based on geophysical methods, they suggested a mechanism of water storage in bedrock depressions, based on a typical "fill & spill" mechanism (Tromp-Van Meerveld and McDonnell, 2006). It should be noted here that the highly cited work of Clow et al. (2003) (108 on webofscience) relies on an (unnoticed) incorrect equation for their recession analysis, leading to a 100 fold overestimation of the aquifer thickness in talus slopes, potentially inducing incorrect conclusions in other studies in the field. What can be retained is that: (i) talus slopes are composed of coarse material and have very high hydraulic conductivity (Muir et al., 2011); ii) a finer layer characterized by high storage capacity may be present if talus slopes cover other landforms such as glacial deposits (Sass, 2006; Baraer et al., 2015); iii) talus slopes play an important role in conveying snowmelt and precipitation and may store water in depressions or in the underlying fractured bedrock(Muir et al., 2011; Liu et al., 2004). ~~Finally, talus slopes should not be confused with lateral moraine deposits since they are much coarser (Rogger et al., 2017).~~ While steep slopes may be influenced by paraglacial mass wasting, if the sediments are located inside the proglacial zone, there is a high chance that a lower layer of glaciogenic material exists below it (e.g. lateral moraine deposits). In that case, the hydrological behavior of such system is likely to be closer to that of a lateral moraine, which is composed of a finer non-sorted diamicton, with a hydraulic conductivity at least an order of magnitude lower as shown in the work of Rogger et al. (2017) or Caballero et al. (2002).

The reviewed studies provide important insights into the functioning of proglacial systems and a qualitative assessment of the hydrological functioning of individual landforms; ~~however,~~ their relative importance and the water connectivity among them remains however largely understudied. Only a limited number of studies propose an integrated description of the hydro-geological behavior of proglacial margins: in the Canadian Rockies a series of papers studied the hydrogeology of different proglacial structures (rock glacier, moraine, talus slope) and were summarized in the work of Hayashi (2020); in the Cordillera Blanca in Peru a suite of studies (Baraer et al., 2015; Gordon et al., 2015; Somers et al., 2016; Glas et al., 2018) focused on the role of groundwater for stream flow in different proglacial valleys and iii) in the Swiss Alps, ~~it is worth mentioning~~ a relatively old review of the hydrological behavior of proglacial landforms by Parriaux and Nicoud (1990), as well as the work in the Damma forefield (Kobierska et al., 2015a, b). Following ~~(~~Heckmann et al., 2016; Vincent et al., 2019~~),~~ there is however still a need for integrative studies that (i) document the hydrological functioning of proglacial landforms with appropriate metrics; (ii) propose a framework to characterize the timing, amount and location of the transmission of different water sources (rain, snow, ice) to these landforms and between each of them; (iii) compare if the documented response of individual landforms can explain the observed catchment-scale behavior in terms of runoff amounts, timing and geochemistry ; (iv) propose a unifying theory for the geomorphological, ecological and hydrological evolution of such rapidly evolving catchments. Within this paper we address the first three of these points.

https://doi.org/10.5194/hess-2022-110
Preprint. Discussion started: 25 April 2022


Hydrology and Earth System Sciences
Discussions

2 Study site and experimental methods

2.1 Site description

With an ice-covered area of about 14 km^2, the Otemma glacier in the Western Swiss Alps is amongst the 15 largest glaciers of Switzerland (Fischer et al., 2014). The glacier is characterized by a relatively flat tongue, which has retreated by about 2.3 km since the little ice age (GLAMOS (1881-2020)) and 50 m year^{-1} since 2015. A recent study suggested an almost complete glacier retreat by 2060 (Gabbi et al., 2012).

Glacial melt used for hydropower production; a~~n~~ Tyrolean-type water intake has been constructed about 2.5 km below the current glacier terminus and is used in the present study as the outlet of what we call the Otemma basin (Fig. 2). It has an area of 30.4 km^2, a mean elevation of 3005 m a.s.l. (2350 m to 3780 m) and a glacier coverage of 45% in 2019 (adapted from GLAMOS (1881-2020)).

The geology of the underlying bedrock is composed of gneiss and orthogneiss from the Late Paleozoic Era with some granodiorite inclusions (GeoCover - Federal Office of Topography). Following a simple slope-based classification (Fig. 2), the main geomorphological structures are composed of apparent bedrock (33.5%), steep slopes (36.6% post-LIA moraines and 19.3% talus slopes), debris cones (6.4%), gently sloping debris fans and morainic deposits (3.3%) and a flat glaciofluvial outwash plain (0.8%). One main subglacial channel at the glacier snout provides water to a large, highly turbid and turbulent stream which quickly reaches a flat outwash plain composed of sandy-gravelly sediments, leading to a braided river network which eventually converges in a more confined channel about 1 km downstream until the catchment outlet. A few tributaries from small hanging glaciers or valleys are also contributing to river discharge during the snow-free season.

2.2 Hydrometeorological data

Since July 2019, an automatic weather station has been installed at the glacier snout and continuously recorded air temperature and humidity, atmospheric pressure and liquid precipitation. Since July 2020, total incoming shortwave radiation was also recorded by the device. Winter solid precipitation data were provided by SwissMetNet, the swiss automatic monitoring network, using information from the Otemma station (2.7 km from glacier snout) or the Arolla station (10 km from glacier snout).

2.3 Hydrological data

Since 2006, hourly river stage was recorded at the water intake corresponding to our catchment outlet ($GS3$, see zoom-in in Fig. 2) by the local hydropower company (Force Motrice de Mauvoisin, FMM); corresponding discharge was estimated using a theoretical stage-discharge relationship provided by FMM. Discharges higher than 10 m^3 s^{-1} are not recorded, which corresponds to the limit of spillway activation of the water intake. We post-processed the data by in-filling data gaps related to regular sediment flushing events (of a duration <1h) with linear interpolation. Winter discharge was also recorded, although a data gap usually occurred from October to December.

https://doi.org/10.5194/hess-2022-110
Preprint. Discussion started: 25 April 2022

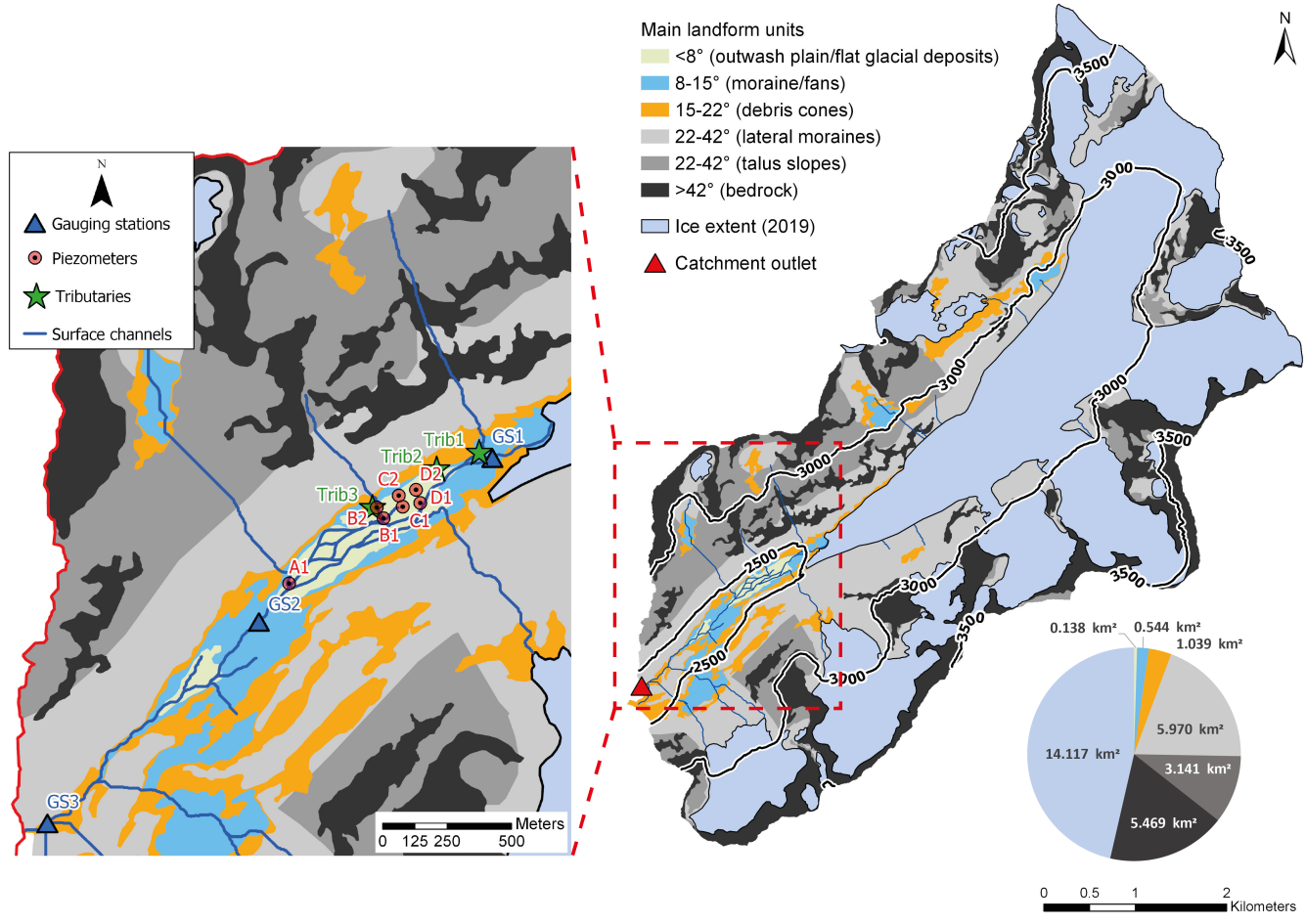

Figure 2. Overview of the Otemma catchment including a first-order, slope-based geomorphological classification following Carrivick et al. (2018). Steep slopes were separated pre-LIA (talus slopes, dark grey) and post-LIA materials (lateral moraines, light grey) using the 1850 swiss glacier inventory (GLAMOS (1881-2020)). The pie chart shows the surface area of each geomorphological unit. The zoom-in window on the left shows the field measurements stations installed between 2019 and 2021. The outwash plain is located between gauging stations 1 and 2 (GS1 and GS2).

Since August 2019, three river gauging stations were installed, one in the vicinity of the glacier snout (GS1), one at the end of the outwash plain (GS2) and one at the catchment outlet (GS3) (see zoom-in in Fig. 2). River stage, water electrical conductivity (EC) and water temperature were recorded continuously at 10 minutes intervals using an automatic logger (Keller DCX-22AA-CTD). Due to the harsh conditions, or low flow conditions during the winter period, there are significant gaps in the data. Periodic EC and discharge measurements were also made in all mapped tributaries or water sources, with a main focus on three representative tributaries along the outwash plain. Finally, 7 piezometers consisting of fully screened plastic tubes were installed at an averaged depth of 1.5 to 2 m in the outwash plain and covered four transects (A to D) perpendicular

https://doi.org/10.5194/hess-2022-110
Preprint. Discussion started: 25 April 2022


Hydrology and Earth System Sciences
Discussions

to the river and reaching the base of the hillslope. Watertable elevation was recorded in each well at a 10 minute interval using SparkFun MS5803-14BA pressure sensors. Sensor bias was verified and corrected by bi-monthly manual groundwater stage measurements.

2.4 Electrical resistance tomography

The depth of the outwash plain sediments was measured by performing multiple transects perpendicular to the river using electrical resistivity tomography (ERT). We measured a maximal sediment depth of around 15 m from the edge of the hillslope where sediment depth was in the range of 2 to 5 m. A few meters below ground, the presence of large buried ice blocks (1 to 30 m wide) was also identified, although its spatial coverage is not clear.

3 Methods

We characterize the hydrological behavior of the above discussed proglacial landforms by assessing their storage-discharge relationship based on recession analysis and a literature review of the timescales of their hydrological response (Sect. 3.1). We then use field-observations of the Otemma catchment, to compare the theoretical storage-discharge dynamics with observations of electrical conductivity, groundwater flowpaths and estimation of hydraulic conductivities (Sect. 3.2). In a third step, we quantify potential storage and discharge capacity for each landform with a simple model (Sect. 3.3).

3.1 Assessing the hydrological response based on aquifer characteristics and recession analysis

We analyze the storage-discharge relationship of selected landforms with classical recession analysis during periods when both water inputs (snow, rain) as well as outputs (evapotranspiration) can be neglected, i.e. during periods when discharge is only related to aquifer storage (Kirchner, 2009; Clark et al., 2009). Following Kirchner (2009) we describe the recession behavior of aquifer storage with a non-linear storage (S)-discharge (Q) function:

$$S = eQ^c, \tag{1}$$

whose derivative, using $\frac{dS}{dt} = -Q$ is given by

$$-\frac{dQ}{dt} = \frac{1}{ce}Q^{(2-c)}. \tag{2}$$

This is usually summarized as $-\frac{dQ}{dt} = aQ^b$, where $a = 1/ce$ is the recession coefficient and $b = 2 - c$ is the slope coefficient (Santos et al., 2018). The release behavior of an aquifer can then be characterized by the rate of change ($-\frac{dQ}{dt}$) versus discharge (Q) and by separating regions where the slope is constant in logarithmic space. In this approach, the form of the aquifer water table can be linked to the shape and physical properties of the landform (Troch et al., 2013). For instance, using some simplifications, the Boussinesq equation (Boussinesq, 1904) proposes a physically-based equation for the temporal variation of the aquifer table along a one directional aquifer and thus allows the discharge to the aquifer table gradients to be linked to aquifer properties (Harman and Sivapalan, 2009a). Many analytical or numerical solutions to the differential equation exist, leading

https://doi.org/10.5194/hess-2022-110
Preprint. Discussion started: 25 April 2022


Hydrology and Earth System Sciences
Discussions

to various values of the recession parameters (a and b), which depend on the defined boundary conditions and assumptions (Rupp and Selker, 2006). Even advanced formula are now proposed, based on complex geometries or hydraulic conductivity distributions. However, some simple and commonly accepted values should provide a good first order estimation of a landform hydrological functioning.

For flat aquifers with homogeneous conductivity, a slope b of 1.5 (c=0.5) is common for the late recession (Rupp and Selker, 2006). Such a value can be obtained using an analytical solution of the Boussinesq equation and leading to the discharge solution (Wittenberg and Sivapalan, 1999; Rupp and Selker, 2005) shown in Eq. (3) & (4):

$$S = eQ^{0.5} \tag{3}$$

$$Q_t = Q_0(1+\alpha t)^{-2} \tag{4}$$

$$\alpha = \frac{Q_0^{0.5}}{e} \approx \frac{K_s h_m}{\phi L^2}. \tag{5}$$

A physical description of α can be proposed (Eq. 5) based on the aquifer conductivity (K_s) and porosity (ϕ), the aquifer length (L) and the aquifer thickness at distance L (h_m) (Dewandel et al., 2003; Rupp and Selker, 2005; Stewart, 2015).

In the case of a significantly slopping aquifer (>10°), a value b=1 is usually proposed for the late drainage (Rupp and Selker, 2006; Muir et al., 2011). In this case, if the aquifer thickness is small enough, the aquifer flux is mostly advective and conducted by the bedrock slope (Harman and Sivapalan, 2009b) so that discharge recession becomes linear (Eq. 6 & 7). Due to the non-linearity of the Boussinesq equation, the parameter α can only be approximated using numerical linearization approaches (Hogarth et al., 2014; Verhoest and Troch, 2000). We propose to use in this study one of the simplest proposed description for α (Eq. 8), similar to the previous one, where only h_m/L (the aquifer slope) is replaced by $sin(\theta)$ where θ is the bedrock slope (Harman and Sivapalan, 2009a; Berne et al., 2005; Rupp and Selker, 2006).

$$S = eQ \tag{6}$$

$$Q_t = Q_0 \mathrm{e}^{-\alpha t} \tag{7}$$

$$\alpha = \frac{1}{e} \approx \frac{K_s sin(\theta)}{\phi L} \tag{8}$$

In both equations, the rate of aquifer decline can be related to a recession constant (α). Its inverse ($1/\alpha$) corresponds to the characteristic response time of the aquifer. It should be noted that this response time can only be partially linked to the mean transit time (McGuire and McDonnell, 2006), since water table variations are governed by advective and diffusive processes, although both travel time and characteristic response seem correlated to flowpath length and gradient (McGuire et al., 2005). By applying the two proposed relationships for a flat (Eq. 5) and a sloping aquifer (Eq. 8) to the various landforms of proglacial catchments, we can assess the timescales at which they will provide water for baseflow. We propose to analyze the recession time needed to decrease the discharge to 50% $\tau_{0.5}$ and to 1% $\tau_{0.01}$. These recession times can be defined for each case as follows:

https://doi.org/10.5194/hess-2022-110
Preprint. Discussion started: 25 April 2022


Hydrology and Earth System Sciences
Discussions

	b=1	b=1.5
$\tau_{0.5}$	$\frac{-ln(0.5)}{\alpha}$	$\frac{\sqrt{2}-1}{\alpha}$
$\tau_{0.01}$	$\frac{-ln(0.01)}{\alpha}$	$\frac{\sqrt{100}-1}{\alpha}$

Despite being a first-order estimation, the proposed recession times are still bound to physical processes and provide a simple framework for comparing the timescales at which different hydrological features provide water; the approach requires only an estimation of the hydraulic conductivity K_s and of the porosity ϕ of the different landforms, as well as the general aquifer geometry.

In Table 1, we compiled the ranges of maximum and minimum hydraulic conductivity values reported in recent studies for various landforms.

Based on this review, we defined realistic aquifer properties (slope, porosity, aquifer length) for each type of landform and calculated the corresponding recession time $\tau_{0.5}$ and $\tau_{0.01}$. Where possible, we also reported the recession constant (α) for comparison and validation of our method. In all cases, these values correspond to the same order of magnitude for different landforms, showing the robustness of the method. It should however be noted that the values are only relevant for the baseflow recession and do not represent the initial fast drainage.

3.2 Estimation of hydraulic conductivity in the outwash plain

In order to estimate the saturated hydraulic conductivity (K_s) of the outwash plain, we use two different methods (see Table 1).

The first method applies the pressure wave diffusion method documented in the work of Magnusson et al. (2014). Given a certain hydraulic diffusivity (D), this method relates the aquifer head variations (h) at a distance x from the stream, to the diel stream stage cycles ($h_{x=0}$) generated by ice melt. It furthermore makes use of a simplified 1D Boussinesq equation, where adjective fluxes are neglected (Eq. 9). This procedure is only valid for relatively flat aquifers with a thick unconfined saturated layer and where evapotranspiration losses can be neglected (Kirchner et al., 2020), which makes this approach well-suited for high elevation outwash plains. By comparing the phase shift (time lag) and the amplitude dampening of the river stage and of the piezometer signals, the aquifer hydraulic diffusivity (D) can be estimated and related to K_s using the aquifer thickness (B) and assuming that the specific yield (S_y) is similar to the aquifer porosity (Eq. 10). This method has the advantage of providing an integrated mean conductivity estimate of the aquifer, as the diffusion is integrated between the stream and the piezometers, avoiding potential over- or underestimations intrinsic to point measurements.

$$\frac{\delta h}{\delta t} = D\frac{\delta^2 h}{\delta x^2} \tag{9}$$

$$D = \frac{K_s B}{S_y} \tag{10}$$

We calibrated the model parameter K_s using a Monte-Carlo approach where we minimized the root mean square error ($RMSE$) and maximized the Spearman rank correlation between observed an modelled piezometer heads. For this analysis, we used the two upstream and downstream piezometer transects (B and D, see Fig. 2) for two periods: during high flow

https://doi.org/10.5194/hess-2022-110
Preprint. Discussion started: 25 April 2022

Hydrology and Earth System Sciences
Discussions
Open Access
EGU

Author	Landform	Method	Aquifer slope [%]	Porostiy [-]	Aquifer length [m]	Slope parameter b [-]	Reported Ks [m s^{-1}] min.	Reported Ks [m s^{-1}] max.	Reported recession constant 1/α in study [days]	Calculated recession constant 1/α [days] min.	Calculated recession constant 1/α [days] max.	$\tau_{0.5}$ [days] min.	$\tau_{0.5}$ [days] max.	$\tau_{0.01}$ [days] min.	$\tau_{0.01}$ [days] max.
Clow et al. (2003)	**Talus slopes**	Recession analysis	25	0.30	200	1	6.50E-03	9.40E-03	-	0.3	0.4	0.1	0.1	0.6	0.9
Caballero et al. (2002)	**Talus slopes**	Kinematic wave propagation	25	0.30	200	1	6.90E-04	2.50E-03	-	1.1	4.1	**0.3**	**1.2**	**2.3**	**8.3**
Muir et al. (2011)	**Talus slopes**	Wave + tracer (chloride)	25	0.30	200	1	1.00E-02	3.00E-02	1	0.1	0.3	**0.0**	**0.1**	**0.2**	**0.6**
Kurylyk et al. (2017)	**Talus slopes**	Kinematic wave propagation	25	0.30	200	1	2.00E-03	2.00E-02	-	0.1	1.4	**0.0**	**0.4**	**0.3**	**2.9**
Caballero et al. (2002)	**Lateral glacial deposits**	Kinematic wave propagation	25	0.25	200	1	2.90E-04		-	8		**2**		**16**	
Rogger et al. (2017)	**Lateral glacial deposits**	Grain size analysis	25	0.25	200	1	2.22E-04		-	11		**3**		**21**	
Langston et al. (2013)	**Glacial deposits**	Mass balance	8	0.25	1000	1.5	3.00E-04	3.00E-03	-	12	121	**5**	**50**	**109**	**1085**
Magnusson et al. (2012)	**Glacial deposits**	Slug test	8	0.25	1000	1.5	6.94E-05	4.86E-04	-	74	521	**31**	**216**	**670**	**4688**
Kobierska et al. (2015)	**Glacial deposits**	Tracer propagation (salt)	8	0.25	1000	1.5	5.15E-04	1.35E-03	0.27 (fast resevoir) 29 (slow reservoir)	27	70	**11**	**29**	**241**	**633**
Winkler et al. (2015)	**Rock glacier**	Tracer propagation (fluorecent)	15	0.30	500	1	7.00E-05	4.60E-02	21 (early recession) 125 (20-80 days) 500 (late recession)	0.3	167	**0.1**	**50**	**0.5**	**334**
Rogger et al. (2017)	**Rock glacier**	Grain size	15	0.30	500	1	5.56E-03		-	2		**0.6**		**4.2**	
Harrington et al. (2018)	**Rock glacier (summer melt)**	Kinematic wave propagation	15	0.30	200	1	5.00E-03	1.00E-02	3 to 4	0.5	1	**0.1**	**0.3**	**0.9**	**1.9**
Harrington et al. (2018)	**Rock glacier (baseflow)**	Spring discharge (Darcy)	15	0.30	200	1	6.00E-05	2.00E-04	14 to 50	23	78	**7**	**23**	**47**	**156**
Robinson et al. (2008)	**Outwash plain (sandur)**	Grain size analysis	2	0.25	1000	1.5	1.16E-04	1.74E-03	-	83	1250	**35**	**518**	**750**	**11250**
Ó Dochartaigh et al. (2019)	**Outwash plain (sandur)**	Pumping tests	2	0.25	1000	1.5	2.89E-04	4.63E-04	-	313	500	**129**	**207**	**2813**	**4500**
Käser et al. (2016)	**Outwash plain**	Pumping test	2	0.25	1000	1.5	6.00E-04	5.00E-03	-	29	241	**12**	**100**	**260**	**2170**
This study	**Outwash plain**	Pressure wave diffusion	2	0.25	1000	1.5	9.60E-04	7.60E-03	-	19	151	**8**	**62**	**171**	**1356**

Table 1. Review of hydraulic conductivity (K_s) reported for proglacial landforms and estimation of related recession time ($\tau_{0.5}$ and $\tau_{0.01}$) based on typical values of aquifer structure (h_L/L, ϕ and L). Maximum and minimum values are given where applicable, red values correspond to point estimation.

during mid-August 2019 and during a lower flow period in mid-September 2019. An additional piezometer "B3" on the same B transect was also used for this analysis. An aquifer thickness (B) of 15 m was chosen based on ERT results and a porosity value (ϕ) of 0.25 from field measurements. The 1D partial differential equation was solved using a central differencing scheme in space and a Crank-Nicolson method in time and imposing the measured river stage variations as a boundary condition. Prior to solving the equation, both river stage and piezometer heads were detrended by substracting the linear trend of each dataset as suggested in the work of Magnusson et al. (2014).

A second independent estimation of the hydraulic conductivity was obtained with salt tracing, using electrical resistivity tomography (ERT) time-lapse with a measurement cycle of about 30 minutes. The ERT device is a Syscal Pro Switch 96 from Iris Instruments. We inject 3 kg of salt dissolved in 15 L of water in a 1 m deep pit in the center of the outwash plain, and record the timing of the passage of the salt plume at a downstream transect (distance 9.38 m) using ERT, similarly to the work of Kobierska et al. (2015a). In our case, we only install one ERT line perpendicular to the groundwater flow consisting of 48

https://doi.org/10.5194/hess-2022-110
Preprint. Discussion started: 25 April 2022


Hydrology and Earth System Sciences
Discussions

electrodes with a 1 m spacing. Hydraulic conductivity can then be calculated solving Darcy's Law for mean pore velocity as follows:

$$v_p = \frac{K_s}{\theta_s}\frac{dh}{dx}, \tag{11}$$

where $\frac{dh}{dx}$ is the aquifer gradient, θ_s is the aquifer porosity and v_p is the mean pore velocity corresponding to the travel distance divided by the travel time of the center of gravity of the salt plume.

3.3 A simple model of proglacial landform dynamics

Table 1 highlights the timescales at which different landforms transmit water. However this analysis does not evaluate the amount of storage or discharge that each landform provides. In order to estimate the relative storage and discharge contribution of different landforms in a catchment, we propose here a simple first-order approach based on the recession theory discussed previously, which we apply to the case of the Otemma catchment. The approach proposes to solve the non-linear storage-discharge relationship ($S_{max} = eQ_0^c$) for discharge, by estimating the recession coefficient e and the maximum storage S_{max}. We propose to estimate e following Eq. (5) or (8) and using realistic hydrological characteristics for each landform: hydraulic conductivity is based on Table 1, while the aquifer slope and length are estimated for each landform based on a 2 m digital elevation model and by manually measuring the averaged landform length (see Fig. 2).

To estimate the maximum storage, we use a simple slope-based classification approach to classify the main hydrological landforms as suggested in the work of Carrivick et al. (2018). Once identified, the potential storage of each landform can be estimated using their total areas (A_i) and an estimation of their sediment thickness. Such a simple approach was already proposed in other similar studies (Hood and Hayashi, 2015; Rogger et al., 2017).

It is however difficult to estimate the maximum aquifer thickness accurately for each landform. To overcome this limitation, we create a simple hydrological model where we simulate a realistic daily water input (Q_{in}) in the form of rain (P_{rain}) and of snow melt (P_{snow}) for each landform and then simulate the evolution of storage (S) during a year, using equations 12 to 14.

$$\frac{\delta S}{\delta t} = Q_{in} - Q_{out} \tag{12}$$

$$Q_{in} = ((P_{snow} + P_{rain})A_i + Q_{glacier})/A_{catchment} \tag{13}$$

$$Q_{out} = \left(\frac{S}{e}\right)^{1/c} \tag{14}$$

where $\frac{\delta S}{\delta t}$ is the change of storage in mm day^{-1}, Q_{in} is the daily water input at time t and Q_{out} is the generated daily output discharge based on the non linear storage-discharge equation. P_{snow} and P_{rain} are the daily snow melt and daily liquid precipitation in mm day^{-1}, A_i is the area of each landform, $Q_{glacier}$ is the daily river discharge from the glacier in liters day^{-1} and $A_{catchment}$ is the total catchment area in m^2. Finally e is the recession parameter estimated based on α (Eq. 5) and c the slope coefficient (1 for slopping aquifers and 0.5 for flatter aquifers).

https://doi.org/10.5194/hess-2022-110
Preprint. Discussion started: 25 April 2022


Hydrology and Earth System Sciences
Discussions

The snow melt input is modelled with a simple snow accumulation routine (snowfall below an air temperature of 2°C) and a degree day model for daily snow melt estimation (Gabbi et al., 2014), with a degree-day melt factor of 4.6 [mm °C^{-1} day^{-1}] when air temperature is higher than 1°C. The melt parameters were fitted by matching the snowline limit during the snowmelt season (Barandun et al., 2018). Winter precipitation were measured at the SwissMetNet Otemma station. For the sake of simplicity, snow and rain inputs are considered to recharge entirely the whole aquifer (no surface flow) and there is no routing or water exchanges between the different landforms.

The only purpose of the model is to provide a first estimate of the storage dynamics based on a realistic water input for each landform independently. In the special case of the outwash plain, an additional glacier melt input ($Q_{glacier}$) is provided, since this is the only landform directly recharged by the river network in Otemma as discussed before. Only a small fraction of the total river discharge was allowed to recharge the outwash plain aquifer, with an infiltration rate of 100 liters sec^{-1} (2% of mean summer discharge) from May to October. Finally the maximum storage (sediment thickness) of the reservoirs cannot be exceeded in any landforms.

This simple model allows an estimation of the water storage and release of single landforms at the catchment scale and should provide a realistic approximation of the volumes of water stored in the superficial proglacial landforms during an entire year.

4 Results

4.1 Catchment-scale winter river recession analysis

To characterize the catchment-scale recession behavior of the catchment, we focus on the discharge recordings during cold months. The focus on this period is required because there should not be any significant water inputs other than groundwater (Kirchner, 2009), when any snow or ice melt stops. Figure 4) shows a plot of the recession rates (dQ/dt) against river discharge (Q). The corresponding recession periods are automatically selected by identifying periods where flow is constantly decreasing for at least 10 days and is extended until the first increase in flow, which usually occurs during spring. The identified recessions typically last between 50 and 100 days. Noise in the discharge data, which creates very small flow increases during the winter, is removed by smoothing the data (moving average with a span of 50% of a given recession period), so that only the averaged trends are analyzed. Finally, all recession points are averaged in bins of an equal number of data points (we selected 100), as suggested in the work of Kirchner (2009). The change in slope for higher discharge values (>0.33 mm day^{-1}, Fig. 3) is probably due to the transition between discharge dominated by ice melt to discharge fed by groundwater. Due to this slope change, we assume that the recession starts when baseflow discharge is smaller than 0.33 mm day^{-1} and higher values are excluded for the linear regression shown in Fig. 3. This linear recession is estimated using the Nonlinear Least Squares method of the "fit" function as implemented in Matlab R2019a.

The estimated regression has a slope of b=1.56. Based on the previous discussion (Sect. 3.1), this value indicates a discharge governed by a rather flat aquifer, although, at the catchment scale, such a slope may arise from an assemblage of hydrological landforms. In any case, a value of 1.56 leads to a quadratic relationship between storage (S) and discharge (Q) where $S = eQ^{0.5}$

https://doi.org/10.5194/hess-2022-110
Preprint. Discussion started: 25 April 2022

Hydrology and Earth System Sciences
Discussions

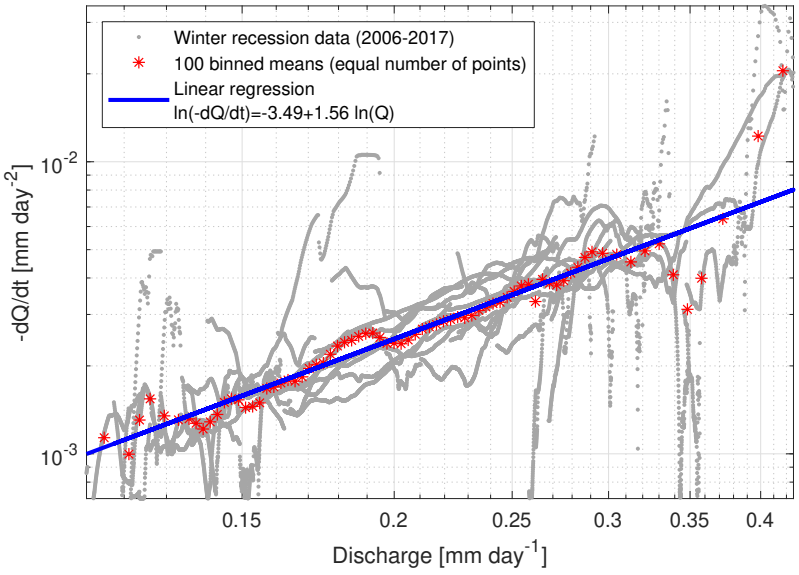

Figure 3. Plot of the smoothed discharge recessions ($-dQ/dt$) against discharge (Q) for all recession periods from 2006 to 2017 (in grey). Shown are also (in red) binned averages, each bin comprising 1% of the datapoints, which show a clear slope change at around 0.33 mm day^{-1}. A linear regression (in the logarithmic space) to all binned values smaller than 0.33 mm day^{-1} is shown in blue. Axes are in logarithmic scale.

and $Q_t = Q_0(1+\alpha t)^{-2}$ (see Eq. 3). Due to the extremely low values computed in Fig. 3, a change in the smoothing process or a change in the maximum baseflow has an impact on the recession. We have tested different processing parameters and assessed the impact on the linear regression; overall, the slope varies between 1.45 and 1.65, which suggests that a quadratic storage-discharge relationship is robust.

Using the same recession periods, the recession trends of each individual years are assessed (Fig. 4) to investigate the evolution of the underlying hydrological processes during this twelve years period, potentially caused by glacier retreat. We fit a power law function on the raw discharge data (without any smoothing) of each winter recession, using the analytical solution of the quadratic relationship as in Eq. 4 with the fitting parameters Q_0 (the maximum baseflow discharge) and e (the recession coefficient).

Based on these annual recession analyses, we can plot the temporal evolution of the catchment-scale baseflow recession constant ($1/\alpha$) and of the estimated maximum baseflow storage, obtained from the storage-discharge relationship, $S_{max} = eQ_0^{0.5}$ (Fig. 5). The temporal evolution of maximum baseflow Q_0 and of S_{max} does not show any clear trend over the twelve years period. Considering the recession constant, there seems to be some decrease in more recent years. The interpretation is however hampered by the data gap in 2010 and by the overall short time period.

Overall, we obtain a relatively consistent estimation of the baseflow storage in the Otemma catchment during winter, with a mean baseflow discharge of 0.34 mm day^{-1}, a mean maximum storage of 42.5 mm and a recession constant ($1/\alpha$) comprised

https://doi.org/10.5194/hess-2022-110
Preprint. Discussion started: 25 April 2022

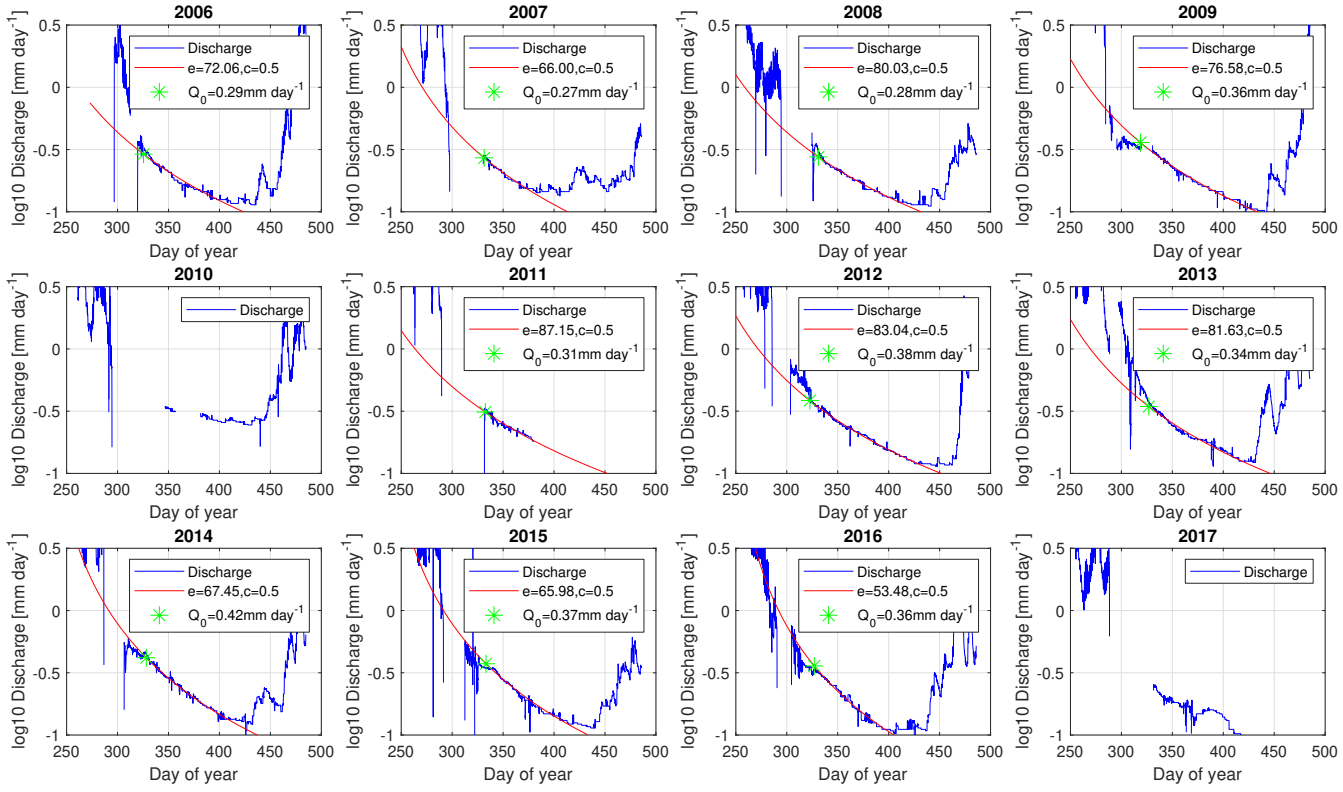

Figure 4. Annual recession analysis at the catchment outlet. The measured discharge is presented in blue (logarithmic scale), the best fit of the power-law regression ($Q_t = Q_0(1 + \frac{Q_0^{0.5}}{e}t)^{-2}$) is shown in red, along with the estimated fitted parameters Q_0 and e. Day of year larger than 365 indicates a recession spanning over the following year. The years 2010 and 2017 have large data gaps and are not shown.

between 90 and 155 days (or a half life recession time $\tau_{0.5}$ between 37 and 64 days). For the interannual analysis (Fig. 3), the corresponding values are 115 days for $1/\alpha$. Finally, it should be noted that at the end of the recession periods in late winter, discharge has usually decreased by a factor of 3 which indicates that the baseflow storage does not completely empty and still retains on average 58% of its maximum storage.

4.2 Water electrical conductivity

4.2.1 Stream observations

In the Otemma catchment, streamflow EC shows strong seasonal and diel cycles driven by snow and glacier melt (Fig. 6). During summer, when discharge is highest, streamflow EC remains very low with small diel variations in the order of 10 to 20 $\mu S/cm$ (zoomed-in box, Fig 6). During this period, EC is strongly negatively correlated with river discharge, with maximum streamflow EC in the morning.

https://doi.org/10.5194/hess-2022-110
Preprint. Discussion started: 25 April 2022

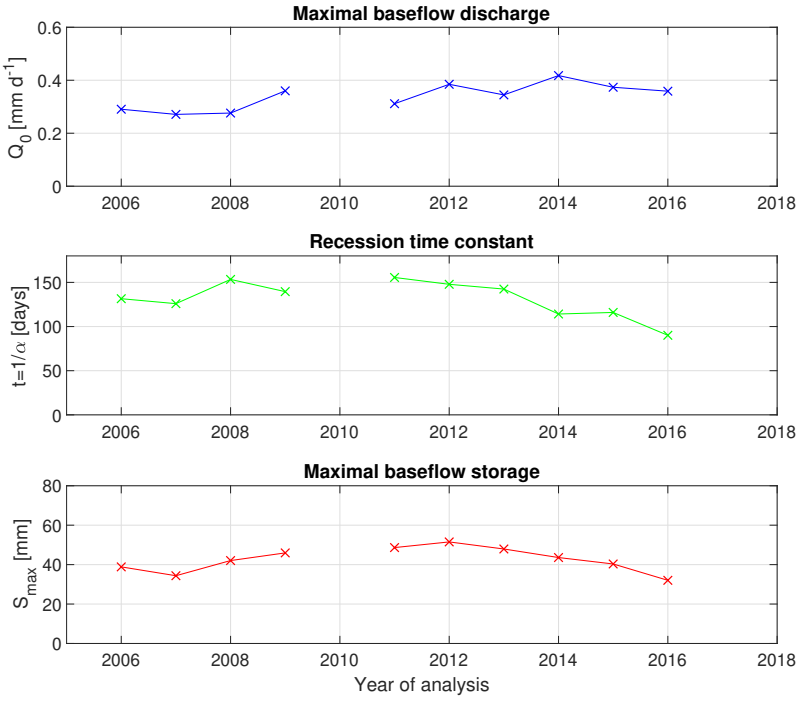

Figure 5. Temporal evolution of recession characteristics obtained from annual recession analysis, showing the results of the best fitted parameters for maximum baseflow (Q_0), recession constant ($1/\alpha$) as well as the first-order estimation of maximum baseflow storage (S_{max}).

There is a small EC increase between the glacier snout (GS1) and the end of the outwash plain (GS2), but hardly any change further downstream (i.e. between GS2 and GS3). This suggests a larger contribution of groundwater or of hyporheic exchanges between GS1 and GS2, i.e. along the outwash plain, than in the downstream part (as also suggested in the work of Kobierska et al. (2015a)). As soon as the river discharge decreases during autumn, a smooth increase of streamflow EC during the whole cold period can be observed, until the onset of snow melt the subsequent year. Although EC could not be measured at the glacier snout during the winter, this steady increase clearly indicates an increasingly larger contribution from groundwater storage compartments, with longer or deeper flow-paths during winter, which correlated well with the discharge recession observed in Fig. 4.

4.2.2 Hillslope and groundwater observations

In order to identify sources of groundwater exfiltration, we monitored the EC of selected landforms as well as of different water sources. The averaged snow-melt EC was $5.1 \pm 2.46\,\mu S/cm$ based on 28 snowpack samples collected during the snow-melt season in the outwash plain and on the glacier surface up to 2850 m a.s.l. Surface ice-melt samples show EC values of $5.7 \pm 4.3\,\mu S/cm$ based on 29 samples; the average rain EC value is $31.6 \pm 11.3\,\mu S/cm$ based on 11 samples. Figure 7 shows the EC values observed in seven piezometers located in the outwash plain as well as of three selected tributaries which represent

https://doi.org/10.5194/hess-2022-110
Preprint. Discussion started: 25 April 2022

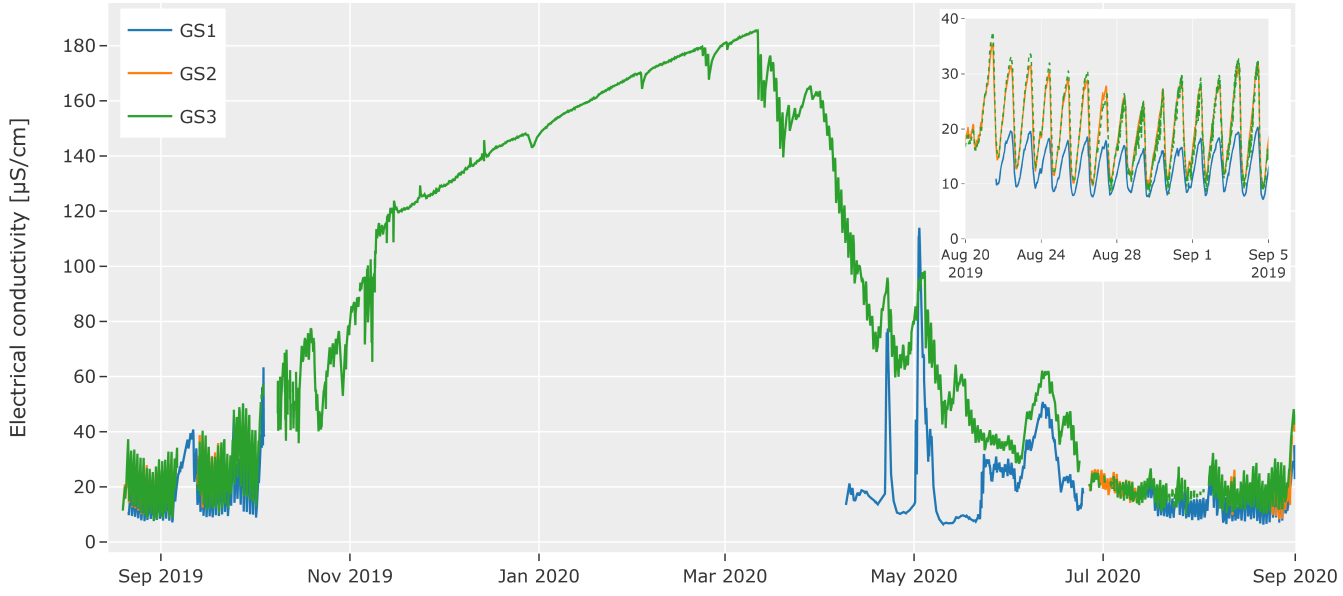

Figure 6. Streamflow electrical conductivity (EC) at the three gauging stations (GS1 to GS3, see Fig. 2 for location). Zoom-in window shows the EC for the first 20 days indicating the similar EC between GS2 and GS3. Large gaps during the winter period are due to sensor failures.

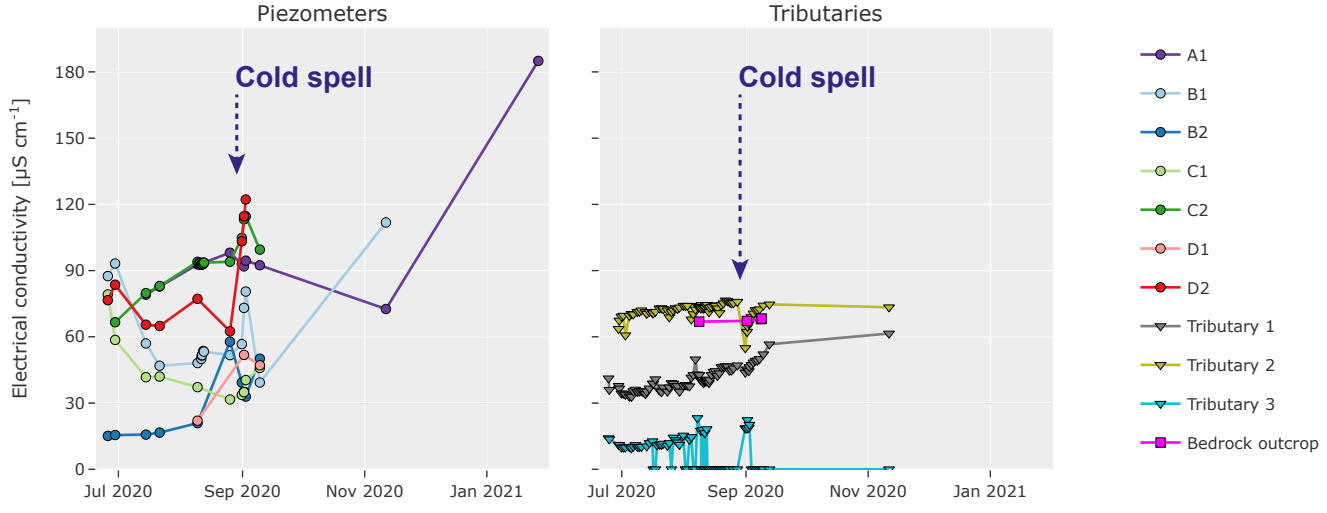

Figure 7. Temporal evolution of EC at seven piezometers (A1 to D2) and in three tributaries as well as one bedrock spring (see Fig. 2 for location). Values of 0 for tributary 3 indicates no surface flow. A cold spell resulting in snow fall over the whole catchment is indicated by the dark blue arrow.

the diversity of values observed along the hillslope and of one water exfiltration at the base of the bedrock outcrop above the tributaries.

https://doi.org/10.5194/hess-2022-110
Preprint. Discussion started: 25 April 2022


Hydrology and Earth System Sciences
Discussions

All tributaries show only limited change in EC during summer, although their concentrations are different. Tributary 1 is located below a higher hanging valley, likely containing buried ice or permafrost with high elevation snow is present during most of the summer, leading to a perennial superficial flow. The relatively low EC values of this tributary seems to indicate a marginal groundwater contribution, with probably only a short contact time between the morainic material and the melted water in the hanging valley in the higher part of the catchment. Tributary 2 exfiltrates from the sediments at the base of the lateral moraine and its EC is only slightly higher than the bedrock exfiltration. This suggests that this tributary is mainly fed by water stored in the bedrock which exfiltrates at the base of the bedrock outcrop, above the lateral moraine, then infiltrates in the coarse sediments and re-emerges at the base of the outwash plain, with only a slightly higher EC, due to a limited chemical weathering.

During the cold spell, accompanied by a heavy rain event (42mm) on the preceding day, a small drop in EC in tributary 2 can be observed and is likely due to an increased water storage in the lateral moraines with low EC, which empties in a few days. Both observations highlight the short residence time of water in the lateral moraine. Tributary 3 maintains very low EC values and becomes dry during August, indicating its direct dependence on snow-melt transmitted by overland flow with hardly any contact time with the sediments.

The EC values measured in the piezometers show much stronger variations, both spatially and temporally. Indeed, there is an increasing lateral gradient away from the stream, indicating strong exchanges with the river. When river discharge becomes lower (cold spell on August 30) or during the winter, piezometer EC becomes larger due to the decreased infiltration of river water or due to lower EC values in the deeper part of the outwash plain. During winter, the water level in all piezometers except A1 dropped below the piezometer depth and accordingly water could only be pumped out of piezometer A1. Here, the EC values more than double between winter and summer, reaching 180 $\mu\mathrm{S/cm}$.

4.3 Groundwater dynamics in the outwash plain

The groundwater head in the outwash plain was monitored continuously in 2019 and 2020 in three transects perpendicular (lateral) to the stream, with one well close to the river, while the second one was located near the hillslope. Figure 8 shows the estimated daily averaged aquifer gradients. Lateral gradients are estimated at two locations, between the upstream piezometers (D1,D2) and between the downstream ones (B1,B2). The slope is mostly comprised between 0 and 0.5% (Fig. 8). Longitudinal gradients parallel to the stream (computed between D1 and C1 (upstream) and between C1 and B1 (downstream)) appear to be much larger, with a slope varying between 1 and 2%.

River stages corresponding to the piezometer transects could not be measured continuously due to the high discharge and unstable sediments; a few isolated measurements show that, in the upper part of the floodplain (B, C, D transects), the river stage is always 10 to 40 cm higher than the groundwater level close to the river, clearly indicating a loosing reach. For the year 2020, the normalized daily averaged discharge is also shown on Fig. 8, showing a very similar dynamic of the discharge and of the upstream longitudinal gradient, although the gradient tends to react with a delay of 1 to 2 days. For both years, the upstream longitudinal gradient seems thus to show a strong dependence on the stream discharge magnitude and starts decreasing in early

https://doi.org/10.5194/hess-2022-110
Preprint. Discussion started: 25 April 2022

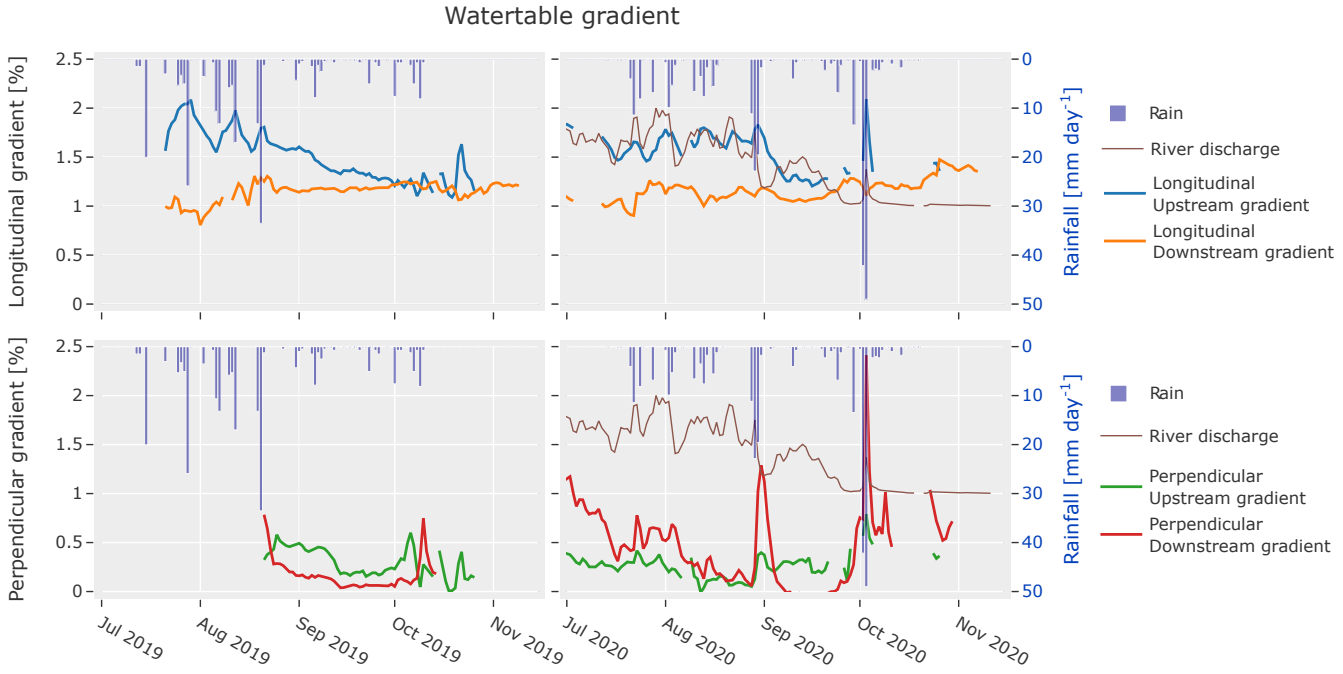

Figure 8. Water table gradients in the outwash plain for summer 2019 and 2020. The upstream longitudinal gradients are estimated between piezometers D1 and C1, the downstream gradient between C1 and B1. The lateral gradients are estimated between "D" piezometers upstream and "B" piezometers downstream and their slope is directed towards the main river. In 2020, the mean daily discharge at the glacier outlet is shown in brown. It was normalized and scaled between 1 and 2 for easier comparison with the gradients. Hourly measured precipitation inputs at the glacier snout are shown by blue bars.

September, i.e. at the moment when discharge is decreasing due to shorter and colder days with reduced ice melt rates. The downstream gradient, about 100m below, is more constant.

The lateral gradients indicate the presence of water contributions from the hillslopes. Indeed, during the year 2020, a consistent decrease of the lateral downstream gradient, almost reaching 0 % in September is linked to the decreased contribution from snow-melt in the small hanging valley above this point. This piezometer is located close to tributary 3 which runs dry early August. Moreover, the EC measured in piezometer "B2" (see Fig. 7), although located far from the river, has a low EC close to the value of snow-melt (median value of 5.1 $\mu S/cm$). The lateral gradient reacts to water inputs, e.g. during a major rainfall event (3rd October 2020) or during a cold spell followed by snowmelt (29th of August 2020), but rapidly returns to its previous state within a few days.

Similarly, the EC of tributary 2 returns to its baseline value on the same time scales of about 5 days after the cold spell. The upstream lateral gradient shows a similar behavior, but much attenuated, with only limited variations. The EC at piezometer "D2" is much higher, suggesting limited recharge from the hillslope at this location. Interestingly, piezometer "A1" (see Fig. 7), shows the highest EC in the floodplain, although it is located at 5m from the river. This seems to indicate a longer flowpath

https://doi.org/10.5194/hess-2022-110
Preprint. Discussion started: 25 April 2022


Hydrology and Earth System Sciences
Discussions

and no exchanges with the river at this location. This observation confirms that groundwater flows in the same direction as the terrain's main slope, is recharged in its upper part and is likely to re-emerge at the end of the outwash plain. This re-emergence results from the underlying bedrock with much lower hydraulic conductivity, which forces water to exfiltrate in the river as the sediment thickness decreases towards the end of the plain.

~~It appears therefore that~~ the aquifer in the outwash plain is mainly recharged in its upper part by the stream and that storage is kept at its maximum during the whole summer (due to glacier-melt), with an aquifer slope governed by the terrain gradient (between 1.2 and 1.5 %). The outwash plain may be partially recharged during the early melt season by snow-melt from lateral valleys, but this effect decreases significantly during the summer. Moreover, such recharge does not seem continuous and occurs mainly at specific locations where upslope water can converge as surface or subsurface flow in the lateral moraines (like in tributary 3) and represents only a minor fraction of the recharge. The dominance of parallel (to the river) flow paths in the outwash plain implies longer flowpaths and residence times and therefore a slower recession, as discussed in the previous section.

4.4 Hydraulic conductivity in the outwash plain

We use two different methods to estimate hydraulic conductivity, the first method is based on the attenuation of a diffusive pressure wave in the aquifer generated by diel streamflow fluctuations and the second uses a salt groundwater tracer to estimate groundwater pore velocity.

Using the diffusion model described in Sect. 3.2, we modeled the diffusion of stream stage fluctuations in the aquifer. Unlike in the work of (Magnusson et al., 2014), satisfying results were obtained using a unique K_s value to simulate the fluctuations of all piezometers along the same transects (see Fig. A1 and A2). The K_s values are summarized in Table 2. Only the estimated lower value for the upper piezometer transect in September 2019 are subject to more uncertainty, as the simulated head variations for piezometer "A1" at 5 meters from the river do not match well the observed results (see Fig. A2b)).

	Hydraulic conductivity K_s [m s^{-1}]	
	High flow condition	Low flow condition
Upstream transect (D1 and D2)	2.5×10^{-3}	0.96×10^{-3}
Downstream transect (B1, B2 and B3)	7.6×10^{-3}	5.6×10^{-3}

Table 2. Estimated saturated hydraulic conductivity [m s^{-1}] of the outwash plain for high flow and low flow conditions during the summer period.

~~From this analysis we observe~~ ~~some~~ spatial variability in hydraulic conductivity and a decrease for lower flow conditions. The low flow K_s value was especially low for the upstream part, which also experienced the largest water head decrease during the autumn season. A decreasing conductivity gradient can be expected with depth, which could affect its water release behavior during low winter baseflow.

https://doi.org/10.5194/hess-2022-110
Preprint. Discussion started: 25 April 2022


Hydrology and Earth System Sciences
Discussions

The second estimation of hydraulic conductivity is performed by monitoring a salt tracer directly in the ground using time lapse ERT (see Sect. 3.2). The passage of the salt plume was identified by a change of resistivity in a well constrained zone of the ERT line (plume radius of about 1 m), with the maximum change occurring 10.5 to 11.5 hours after injection. Using a travel distance of 9.38 m, we obtain an average pore velocity v_p of 2.37×10^{-4} m s^{-1}. The corresponding aquifer gradient between 3 piezometers (one 1m upstream of the injection point and two along the ERT line) has a maximum slope of 1.7%. The mean porosity can be estimated to be around 0.25, based on five saturated water content measurements (using a Decagon 5TM device) at different locations in the outwash plain. Based on these values, we obtain an estimated hydraulic conductivity of 3.48×10^{-3} m s^{-1}.

The surface hydraulic conductivity estimated with the salt tracer approach leads to an estimation of the hydraulic conductivity close to the mean of the values estimated with the diffusion model (4.165×10^{-3} m s^{-1}). Our estimations of the hydraulic conductivity are slightly higher than in a previous study for a similar but older alluvial system (Käser and Hunkeler, 2016) and one order of magnitude larger than for an older sandur (Ó Dochartaigh et al., 2019). It should be stressed that the estimation using the diffusion method is mainly valid for a homogeneous aquifer with constant diffusivity, which is likely not the case in reality. The estimated hydraulic conductivity is thus rather a mean value with depth, although the conductivity at the surface may be somewhat larger. Finally, due to the sedimentological structure of such an outwash plain, composed of fluvially reworked layers of silty sand and gravels, hydraulic conductivity is spatially variable and some regions containing coarser materials are likely promoting preferential flow paths potentially allowing for a faster averaged aquifer velocity than our estimates. Such zones can be visually identified in the field, where water preferentially exfiltrates into kettle holes.

4.5 Groundwater storage in hydrogeological landforms

We analyse the relative contribution and the timescales at which each hydrogeological landform provides water based on the model described in Sect. 3.3, which yields an estimation of the storage, of the response time of each unit and of the landform area. A realistic estimation of the recession constant ($1/\alpha$) is taken from the averaged hydraulic conductivity values following Table 1 and adapted to the case of the Otemma catchment. Based on the literature for lateral moraines (Caballero et al., 2002; Rogger et al., 2017), we selected K_s to be smaller for lateral moraines and for debris cones than for flatter moraines (Kobierska et al., 2015a), which probably reflects the lesser degree of compaction at the valley bottom. We separate talus slopes from steep lateral moraine as talus slopes material is coarser and is mostly only covering morainic material below the Little Ice Age line. For the outwash plain, the averaged hydraulic conductivity estimated in the previous section was used. The flatter morainic deposits (moraines and fans with a slope between 8-15°) have a similar hydrological response as debris cones (slope between 15-22°) in terms of response time as illustrated by a similar recession constant $1/\alpha$; this results from the opposite effects of aquifer length and of K_s. Due to this similar hydrological response, we merge landforms between 8° and 22° (moraines and debris cones) together into a single "moraine" landform class for the following approach. All retained parameters for all landforms are summarized in Table 3.

For the estimation of landform saturation, total liquid water inputs are taken from the measured liquid precipitation in the Otemma catchment and from estimated melt (see Sect. 3.3) during the year 2020. Rainfall amounts to a total of 273 mm and

https://doi.org/10.5194/hess-2022-110
Preprint. Discussion started: 25 April 2022

Hydrology and Earth System Sciences
Discussions
Open Access
EGU

	Landform area (A_i) [km^2]	Slope [%]	Porostiy [-]	Aquifer length [m]	c [-]	K_s [m s^{-1}]	$1/\alpha$ [days]
Talus slope	3.141	50	0.30	250	1	5.0E-03	0.23
Lateral moraine	5.970	50	0.25	250	1	3.0E-04	5.4
Debris cone	1.04	27	0.25	250	1	3.0E-04	9.3
Moraine/fans	0.54	14	0.25	500	0.5	1.0E-03	10.4
Outwash plain	0.14	2	0.25	1000	0.5	4.0E-03	36.2

Table 3. Estimated saturated hydraulic conductivity [m s^{-1}] of the outwash plain for high flow and low flow conditions during the summer period.

615 snow melt to 1266 mm of water equivalent (see Fig. 9a). Figure 9b) shows the resulting estimated maximum storages for each landforms.

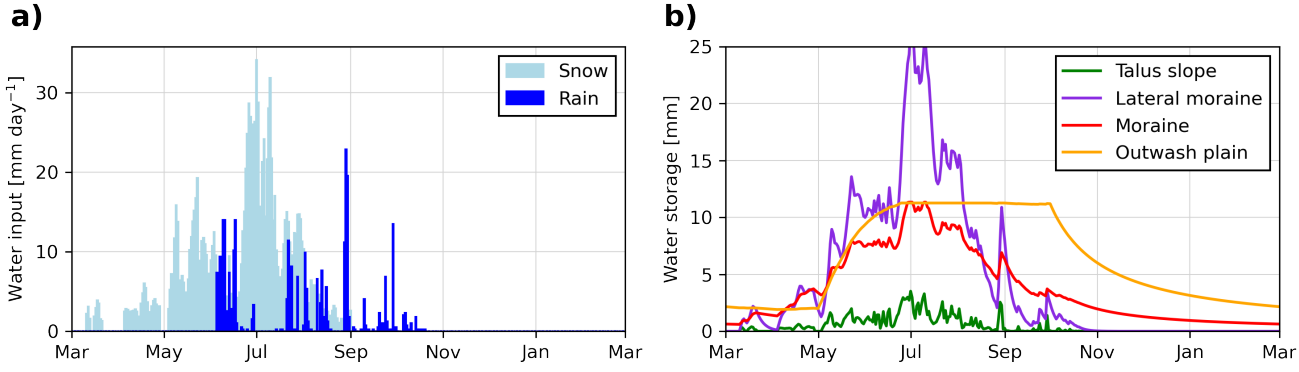

Figure 9. a) Measured precipitation input at glacier snout [mm day^{-1}] and mean snow melt input simulated with the simple degree day approach [mm day^{-1}]. b) Evolution of the groundwater storage of four geomorphological landform units based on the model described in Eq. 12 to 14.

The resulting maximum storage in the moraines is 11.3 mm or a maximum aquifer thickness of 0.87 m during peak snow melt. The storage in the outwash plain gradually increases due to constant recharge from the river and rapidly reaches its maximum storage of 11.3 mm (or an aquifer thickness of 10 m). The lateral moraines show a very flashy storage response
620 linked to their short recession constant, so that their storage reaches 27.2 mm during snow melt, corresponding to an aquifer thickness of 0.55 m. Due to their very low retention capacity, talus slopes only transmit water and their storage is low (3.5 mm) with a maximum aquifer thickness of 0.11 m. After peak snow melt, storage decreases in both lateral and flatter moraine landforms and only the outwash plain maintains high storage due to the river discharge. However, by the month of November, the total remaining storage becomes very limited with only 5 mm remaining from the outwash plain.

https://doi.org/10.5194/hess-2022-110
Preprint. Discussion started: 25 April 2022


Hydrology and Earth System Sciences
Discussions

This result is in contradiction to the catchment-scale recession analysis (Fig. 5), which results in a storage estimate of 40 mm, along with a recession constant of more than 100 days. Accordingly, the landform-based analysis seems to miss a relatively important storage compartment (see Sect. 5.1.5).

5 Discussion

5.1 Groundwater storage and release functions of the main geomorphological features

The literature review as well as our data-analysis in the Otemma catchment have shown that the landform- as well as the catchment-scale hydrological response critically depend on both the sediment structure defining K_s as well as on the landform characteristics in terms of slope and aquifer flow path length. These key properties can then be combined to estimate an averaged response time of each landform. It should be noted that the storage-release behavior may be more complicated when considering more complex aquifer geometries (Berne et al., 2005), heterogeneous landform with varying physical propriety for K_s and ϕ, as well as preferential flow paths (Harman et al., 2009) and non-stationary processes (Benettin et al., 2017). Nonetheless, we believe that our approach is relevant to highlight the main hydrological dynamics and provides a valuable first-order estimation of the storage-release behavior allowing for the establishment of a sound perceptual model (see Sect. 5.2). Prior to this model, we first discuss and summarize hereafter what new insights we gain from our case study on the hydrological functioning of the main classes of geomorphological landforms.

5.1.1 Talus slopes

Due to their coarse aquifer structure leading to a fast hydraulic conductivity, talus slopes have short recession constants of the order of a day, leading to a rapid transmission of water and little water retention. If a less conductive layer exists at the bottom of the talus, most studies have only reported a few centimeters of water saturation with still relatively high conductivity (Muir et al., 2011; Kurylyk and Hayashi, 2017), which should not lead to significantly longer water retention. As highlighted with our electrical conductivity (EC) data in the Otemma catchment, talus slopes do not store water but transmit it from other landforms or from the underlying fractured bedrock (McClymont et al., 2011; Harrington et al., 2018). Groundwater storage is likely discontinued and occurs in pockets at the base of the talus (fill and spill mechanism (Muir et al., 2011)).

5.1.2 Steep lateral moraines

Steep lateral moraines may present glacial deposits of the order of tens of meters (Rogger et al., 2017) and their structure is that of a diamicton containing a significant part of fines with some degree of consolidation, leading to lower hydraulic conductivity than talus slopes. Even though their structure is steep, due to a slower conductivity, they may retain water at a timescale of a week. Their response remains relatively flashy and the amount of potential storage is mainly driven by the rate of snow melt in the early summer season. In our basic model, we assumed an homogeneous recharge, which is unlikely in the later mid-summer season, when snow melt mainly occurs in the upper, flatter part of the catchment or in hanging valleys, and when both surface

https://doi.org/10.5194/hess-2022-110
Preprint. Discussion started: 25 April 2022


Hydrology and Earth System Sciences
Discussions

and subsurface melt water responsible for its recharge are likely concentrated in gullies or other zones of flow convergence due to the bedrock topography. The amount of recharge of steep lateral moraines is thus likely dependent on the frequency of flow convergence upslope; the more concentrated is the upslope flow, the less recharge occurs. Thus, the estimated storage of such landforms due to snow melt is likely not as large as estimated here (25 mm), as only a fraction of this landform is located above zones of snow-melt induced recharge. They nonetheless have the potential to store significant amount of rain water, at least in the Otemma catchment, as they cover a significant part of the proglacial zone (20%), although they rather act as a buffer, only redistributing water on a timescale of a week. Finally, if their grains are highly cemented, water may only infiltrate until the interface with an upper coarser part where sediments are less compacted due to gravitational (similar to talus slopes) or fluvial reworking. This may be partially the case in the Otemma catchment, as observations in the tributary 2 seem to indicate a very fast water transmission from either the bedrock directly, or upper valleys. At this point we can only postulate that tributaries emerging from the lateral moraines do not infiltrate completely in the morainic materials and a fraction is rather transmitted in the superficial sediment similar to talus slopes. However, it is also likely that water which does infiltrate into the lateral moraine directly enters the outwash plain underground, making direct observations not possible as suggested in the work of Baraer et al. (2015).

5.1.3 Glacial deposits

Flatter glacial deposits, such as alluvial fans or melt-out till moraines have a similar structure to steeper moraines but are usually less cemented and may present an eluviation of fines, leading to a somewhat greater hydraulic conductivity (Langston et al., 2011; Ballantyne, 2002). In Otemma, those mildly sloping structures are dominated by moraine deposits and their recession constant was estimated to be twice as large as the one for steeper moraines. Although their recession is only two-times longer, their flatter aquifer gradient results in a slower decrease of storage characterized by a quadratic recession (c=0.5, see Eq. 3). Their capacity to sustain baseflow however dependents strongly on the amount of water recharge during the snow melt period. As earlier snow melt is expected in the future, their storage capacity will likely be strongly reduced on time scales of weeks after peak snow melt. Moreover, those flat structures only cover a small area so that the total amount of rainfall they can store during a storm is limited. Where glacial deposits are connected to a more constant source of water such as ice melt, storage may remain high throughout the summer (Kobierska et al., 2015b), and they will function similarly to an outwash plain as described hereafter. In the case of the Otemma catchment, the usual thickness of these sediments is on the order of tens of meters, making direct groundwater observation at their base challenging. No clear changes in EC was observed in summer beyond the outwash plain (between GS2 and GS3), a section where morainic material is present. Due to the low residence time of water in such landforms (days to week), snow-melt or rain fed groundwater exfiltrating from glacial deposits do not have a long contact time with the sediments limiting chemical weathering and will thus only show a slight increase in EC, which may be similar to the river EC. It is therefore likely that even if those glacial deposits exfiltrate water, it will not lead to any changes in the streamflow EC along this reach.

https://doi.org/10.5194/hess-2022-110
Preprint. Discussion started: 25 April 2022


Hydrology and Earth System Sciences
Discussions

5.1.4 Outwash plains

As observed in the case of the Otemma catchment and as also reported in the literature (Mackay et al., 2020), outwash plains show strong surface water-groundwater interactions, which maintain near saturation conditions far after the peak of snow melt as long as some limited glacier melt is provided. Moreover, when ice-melt decreases in winter, outwash plains may provide some baseflow due to their longer recession constant (about 35 days). If their current role to maintain baseflow is clearly limited due to their very small areal extent in alpine catchments, future glacier retreat will extend their area, especially where overdeepenings can be filled with sediments. Finally, together with earlier snow melt in a warming climate, their role in providing baseflow during drought conditions is likely to become increasingly important in the future.

5.1.5 Missing storage

From the above comments and the simple model summarized in Fig. 9, it appears that the current capacity of the geomorphological landforms to store water is limited to the melt period, with the exception of the outwash plain. Nonetheless, on the basis of baseflow recession analysis in the Otemma catchment, we estimated a potential groundwater storage of the order of 40 mm.

This missing storage cannot be identified clearly with the current approach but some hypotheses can be formulated for further investigation. The first hypothesis is that the remaining baseflow recession in winter is actually not due to a storage unit, but rather to some residual snow melt or basal melt at the glacier bed. The observed increase in EC during winter does not agree well with this hypothesis, except if the melt actually transits through other landforms giving sufficient time to acquire solutes by the weathering of bedrock or sediment.

The second hypothesis is the contribution from a groundwater reservoir underneath the glacier itself. Previous studies have however predicted a rather rocky or mixed glacial bed in this area (Maisch et al., 1999), with limited till thickness on the order of tens of centimeters and with a likely discontinued nature (Harbor, 1997). A large enough reservoir (four times the current outwash plain) could exist in a large glacial overdeepening but it is unclear if sufficient sediment would accumulate in such a pocket based on the sediment export capacity of the glacier.

The third hypothesis is that the storage occurs mainly in the bedrock and that sufficiently short flowpaths allow this storage to drain during the winter. This hypothesis is more likely since large fractures may occur due to glacier debuttressing (Bovis, 1990; Grämiger et al., 2017) and groundwater seepage through deep fractures probably occurs underneath other landforms and cannot be clearly identified. Moreover, some studies have reported similar catchment scale storage in elevated catchments, although it is usually not clearly associated with a distinct hydrological unit. In particular, in a similar highly glaciated catchment, the work of Hood and Hayashi (2015) reported a peak catchment-scale storage in spring of 60 to 100 mm. Moreover, the work of Oestreicher et al. (2021) modelled an estimated catchment-scale storage change of 70 mm in a similar swiss glaciated catchment, which they could relate to a deep borehole water head change (Hugentobler et al., 2020), leading to a realistic porosity estimation of 0.5 %. Such estimates represent the peak spring storage, accounting for all storage units, and not only the winter storage estimated in our study. Based on the rough estimates of Fig. 9, the peak summer storage estimated is 26 mm for morainic material and the outwash plain and 25 mm for the steep lateral moraines, which, combined with a bedrock

https://doi.org/10.5194/hess-2022-110
Preprint. Discussion started: 25 April 2022

Hydrology and Earth System Sciences
Discussions

storage of 40 mm, would result in similar numbers. It remains unclear if bedrock exfiltrations could increase the winter stream electrical conductivity up to 185 $\mu S/cm$, since the measured bedrock leakage had an EC of 60 to 80 $\mu S/cm$. Such a high electrical conductivity was only observed in piezometer "A1" during winter (Fig. 7) so that it is likely that part of the winter baseflow transits through the outwash plain before reaching the main stream, either through subsurface bedrock exfiltration into the outwash plain and/or through a residual upstream discharge that infiltrates into the outwash plain and re-emerges in its downstream part, as showed in the work of Malard et al. (1999) and Ward et al. (1999).

Based on the above discussion, we propose to allocate the missing storage to bedrock storage with a maximum storage of 40 mm, which we can then add to our previous model (Eq. 12) with a recession constant ($1/\alpha$) of 100 days to reflect the baseflow recession analysis. The resulting baseflow of each landform is shown in Fig. 10.

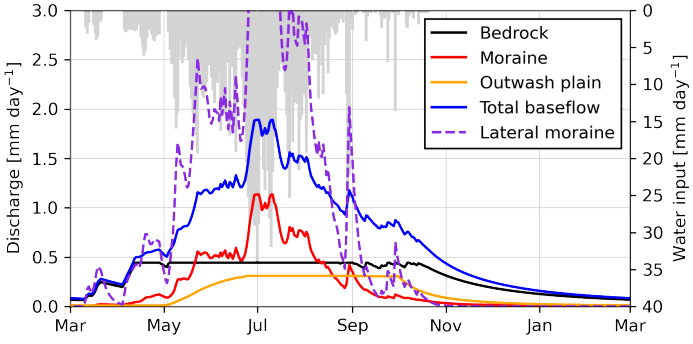

Figure 10. Evolution of modelled groundwater baseflow discharge of different hydrogeomorphological landforms. Total baseflow represents the sum of outwash plain, moraines and bedrock discharge; steep lateral moraines are also plotted but are not considered into the sum of baseflow due to their fast response. Simulated total water input (snow melt and rain) are plotted in grey.

5.2 A sound perceptual model of a proglacial catchment

We summarize here the gained insights into a perceptual model of the hydrological functioning of the Otemma proglacial catchment, with a focus on storage-discharge behavior as well as hydrological connectivity between landforms.

Our results indicate clearly that winter baseflow is governed by a storage reservoir not linked to superficial landforms, with the exception of the outwash plain, which provides a limited baseflow. It also appears that during strong summer rainfall events, the moraine landforms only provide water over short time scales. Lateral steep moraines provide quite important discharge during such events, but their storage becomes quickly exhausted (around a week later); flatter moraines do not react strongly.

While the estimates should not be taken as an exact representation of groundwater storage and release, they do allow some insights into the relative magnitude and timing of the contribution of different landforms (and of associated water storage compartments) to baseflow, which we propose to summarize in the perceptual model sketched in Fig. 11. In this representation, the storage shares are taken from our Otemma results and the result from our model (Eq. 12) augmented with an additional "missing" storage to represent winter baseflow (see Sect. 5.1.5). The glacier storage share represents the mixed discharge

https://doi.org/10.5194/hess-2022-110
Preprint. Discussion started: 25 April 2022

Hydrology and Earth System Sciences
Discussions

leaving the glacier outlet and is an undefined mix of ice and snow melt as well as of any liquid rain transiting through the glacier. In order to better represent the seasonal evolution of the storage of each landform and of its saturation, a maximum theoretical storage for each landform is used to represent its saturation level and a "dry" storage is represented when the landform is not fully saturated. Steeper lateral morainic deposits were merged with the "moraine" landform since they show relatively similar response.

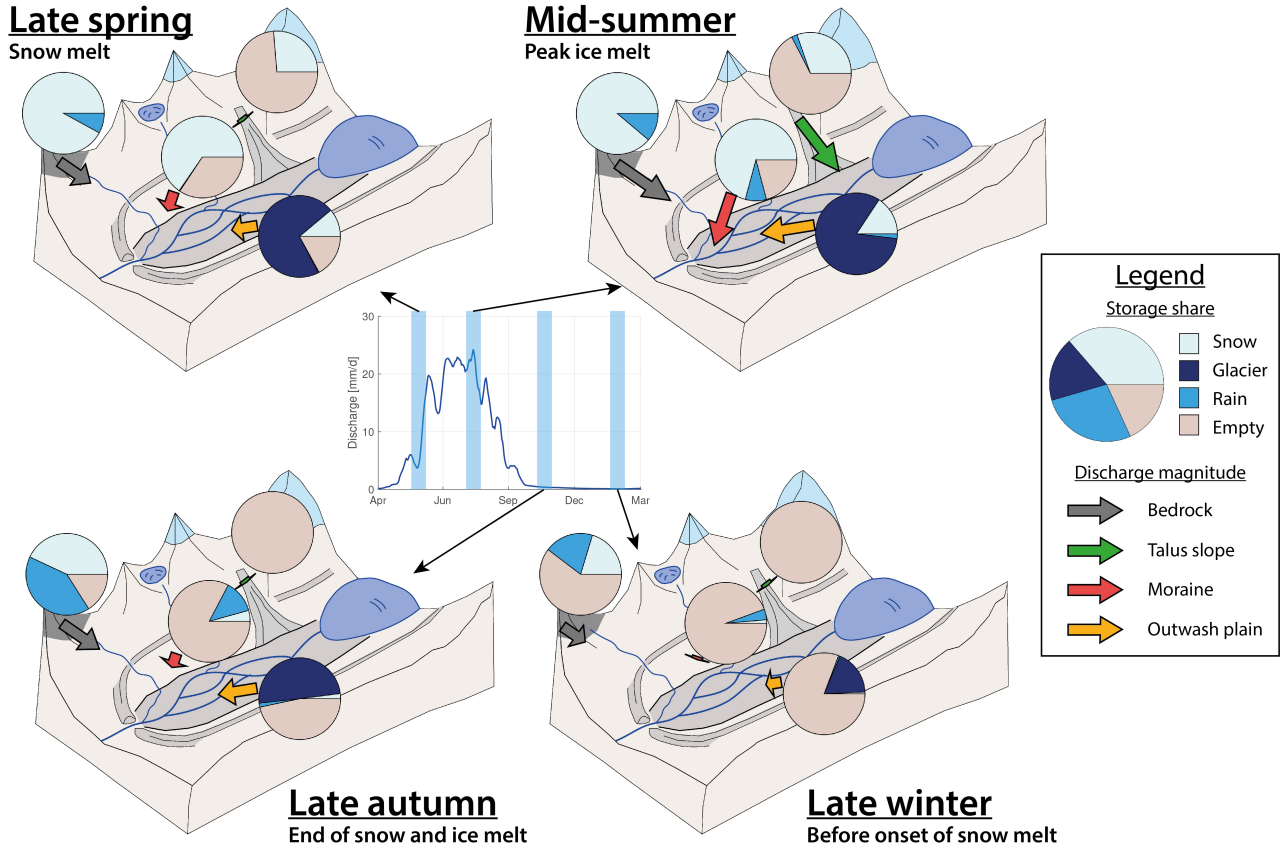

Figure 11. Perceptual model of groundwater dynamics in the Otemma proglacial catchment during four key hydrological periods. The central hydrograph represents the mean daily catchment-scale river discharge for the year 2015. The pie charts represent the identified share of water storage for the four main landforms. Dry storage represents the percentage of aquifer non-saturation from the estimated maximal storage (Sect. 4.5), which is 40 mm for bedrock (missing storage); 3.5 mm for talus slope and 11.3 mm for moraine and 11.3 mm for outwash plain. The length of the arrows represents the relative magnitude of the baseflow discharge of each landform.

While our approach identifies the relative size and seasonal hydrological response of proglacial landforms, we use a very simplistic recharge model. In reality, hydrological connectivity from the water sources and between landforms will ultimately drive the amount of actual recharge. Due to the coarse and barren nature of the sediments in proglacial landforms and the limited presence of soils, it can be expected that any water inputs infiltrate into the sediments (Maier et al., 2021a). It has

https://doi.org/10.5194/hess-2022-110
Preprint. Discussion started: 25 April 2022

also been shown that groundwater flow is driven by the bedrock topography underneath the landform, where a strong change in hydraulic conductivity drives the water downslope (Hayashi, 2020; Vincent et al., 2019). We can therefore assume that a primary recharge occurs directly at the location of the water input, will percolate until the bedrock and will then be directed downslope. In the case of snow melt, this recharge will gradually move upslope as snow melts during the summer, a zone where talus slopes and bedrock are frequent. Water will rapidly be directed downslope at the bedrock interface and directed in zones of bedrock depression, concentrating the flow as discussed in Sect. 5.1.2. Water may also reach a flatter zone in hanging valleys, where flatter morainic material may be present in rock overdeepenings, which likely act as a primary immobile storage, where groundwater only overflows above the bedrock similarly to a fill and spill mechanism (Tromp-Van Meerveld and McDonnell, 2006). The concentrated groundwater flow eventually reaches either lateral morainic material or a flatter moraine or outwash plain and acts as point recharge, so that only parts located below a zone of bedrock convergence will receive recharge. Similarly, glacier melt recharge will mostly occur along the reach of the glacial stream at the valley bottom and will maintain high groundwater storage in outwash plains or flat moraines only.

Finally, bedrock stores water in fractures and a rapid bedrock recharge occurs in the early snow melt season (Oestreicher et al., 2021). Since bedrock is ubiquitous below the sediments, precipitation may there represent an important recharge as illustrated in the pie chart in Fig. 11, although the rate of infiltration is not clear. While locations of bedrock exfiltrations are difficult to observe, winter baseflow suggests that an underground recharge from the bedrock occurs into the flatter moraine and outwash plain sediments.

6 Conclusions

This study attempted to bridge the gap between the catchment scale response of an elevated glaciated catchment and the hydrological behavior of its landforms, relying both on a detailed literature review of the current knowledge of such environments and on the Otemma case study in the Swiss Alps. The quantitative analyses are simple and are based on a rough estimation of the hydrogeological response of different landforms. Nevertheless, the analysis framework can identify the order of magnitude and of timing of the contribution of the different landforms and is readily transposable to other case studies. The resulting perceptual model provides a realistic representation of the main drivers of the groundwater dynamics of a proglacial catchment, which can serve as a blueprint for future experimental works as well as hydrological model development. One clear uncertainty lies in the estimated hydraulic conductivities per landform, in particular their variability in space and depth. Also, we had to attribute a large part of the groundwater storage to an unidentified compartment, which is likely partially due to a bedrock compartment, but could also be due to a combination of melt water and a subglacial compartment. Future research is needed to specify the very nature of this groundwater storage.

We have shown that superficial geomorphological landforms have a relatively limited capacity to store or release water at timescales longer than a few days, partly because of steep slopes but also due to the generally high hydraulic conductivity. In the future, two main changes can be expected. Firstly, with increasing glacier retreat, the extent of flatter landforms at the valley bottom will increase and may accumulate sufficient sediments to create new outwash plains or flat hummocky moraines

https://doi.org/10.5194/hess-2022-110
Preprint. Discussion started: 25 April 2022


Hydrology and Earth System Sciences
Discussions

that would increase the overall groundwater storage. It remains unclear how much sediments are produced with decreasing glacier volumes and to which extent sediment will be rather deposited or transported more downstream (Lane et al., 2017; Carrivick and Heckmann, 2017). Secondly, with increasing succession time to allow vegetation growth, the formation of soils with enhanced organic matter content and finer soil texture are expected, which will enhance water retention and modify the surface hydraulic conductivity (Hartmann et al., 2020). Recent studies on the evolution of morainic structure have shown that limited changes occured on time scales smaller than a millennium, with a slight decrease in hydraulic conductivity (Maier et al., 2020, 2021b). Thus, the impacts of soil-vegetation development are likely to be greater where there is accumulation of sands, silts and clays than for landforms in proglacial margins containing gravel and coarser deposits and the development of biofilms can start to modify water retention substantially (Roncoroni et al., 2019). Finally, the ecological feedback of vegetation development on bank stabilization may also play a role in limit sediment export and promote less geomorphological changes (Miller and Lane, 2018) which may preserve the present geomorphological landforms, although riverbed erosion may increase.

The presented framework to analyze the hydrological behavior of selected landforms based on water level and electric conductivity (EC) recordings is readily transferable at relatively low cost to other proglacial catchment. Our EC recordings underline its large variability between the landforms and spatially across the outwash plain, in addition to strong variations with changing groundwater heads. This observation shows that simple mixing models based on few observations of groundwater electrical conductivity in selected sources are likely not representative of the contribution of each landforms and may provide very erroneous estimation of groundwater contribution.

More sophisticated tracer work could complement these analyses in the future. We in particular think of stable water isotopes that could provide interesting insights into the relative share subsurface recharge resulting from snow and rain over the season. The use of other geochemical tracers (Hindshaw et al., 2011; Gordon et al., 2015) or even noble gases (Schilling et al., 2021) could provide further insights into the temporal evolution of the baseflow as well as better constrain the length or travel time of certain flowpaths.

Code and data availability. Field data are available on Zenodo (https://zenodo.org/communities/otemma). Weather data are available under (Müller, 2022a), piezometer data under (Müller, 2022b), river data (Müller and Miesen, 2022) and ERT data under (Müller, 2022c).

The code to reproduce the recession analysis (see Sect. 4.1) was written in matlab using the published data. The code for the simple storage-discharge model (see Sect. 4.5) was written in python using Jupyter Notebook. Both codes are available in supplementary material.

Author contributions. T.M. conducted all the data collection and data analysis, produced all the figures and wrote the manuscript draft, including the literature review. B.S. proposed the general research topic and acquired the funding. S.L. and his team organised all field work logistics. B.S. and S.L. jointly supervised the research and edited the manuscript draft version. All authors have read and agreed to the current version of the manuscript.

https://doi.org/10.5194/hess-2022-110
Preprint. Discussion started: 25 April 2022

Hydrology and Earth System Sciences
Discussions

Competing interests. The authors declare that there is no conflict of interest. One co-author is a member of the editorial board of Hydrology and Earth System Sciences.

Acknowledgements. The authors also thank Prof. Christophe Lambiel and Prof. James Irving (University of Lausanne) for lending the ERT device as well as Dr. Emily Voytek (University of Lausanne) for acquiring the first ERT data in the Otemma forefield in 2019. T.M. thanks all students and PhD students from the AlpWISE group at University of Lausanne and in particular Floreana Miesen who participated in field data collection at the Otemma glacier forefield.

Appendix A: Diffusion model analysis

Figure A1 and A2 show the results of the diffusion model using the optimal diffusion parameter for both upstream and downstream piezometer lines (see Sect. 4.4).

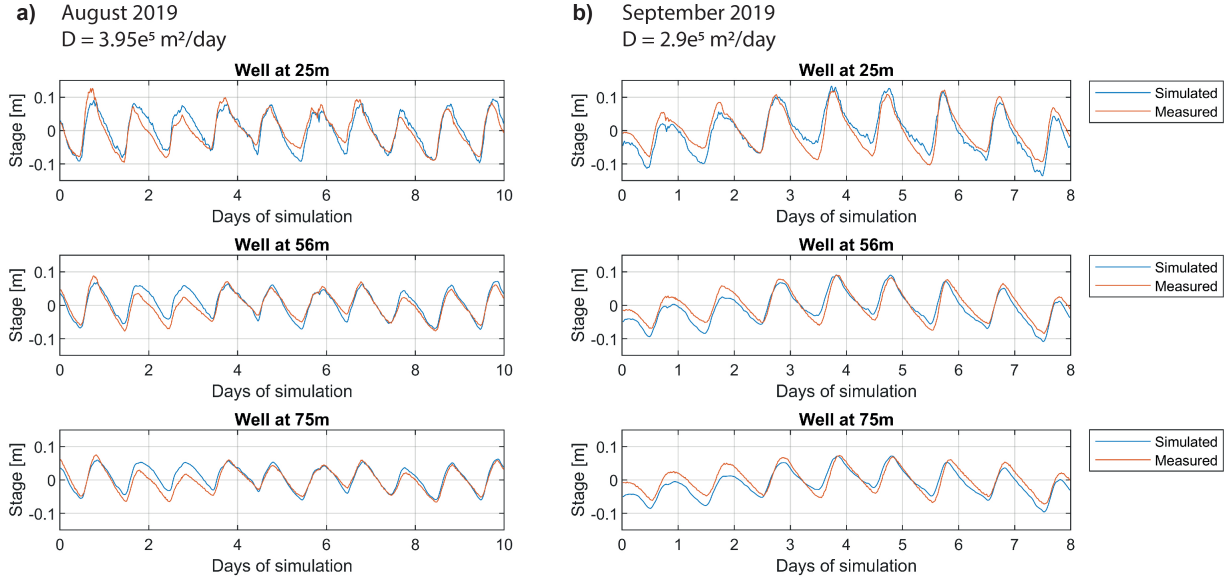

Figure A1. Measured and simulated water head variations for piezometers along the downstream transect "B" for the best calibration of the diffusion parameter D and for a) the high flow condition in August 2019 and b) lower flow condition in September 2019.

https://doi.org/10.5194/hess-2022-110
Preprint. Discussion started: 25 April 2022

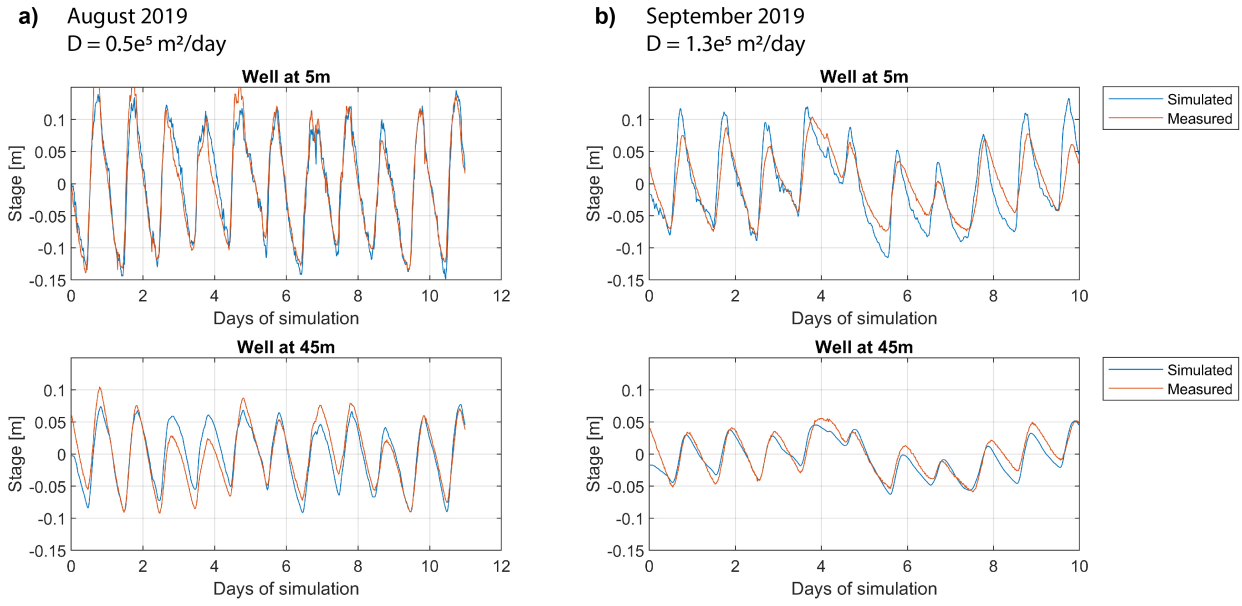

Figure A2. Measured and simulated water head variations for piezometers along the upstream transect "D" for the best calibration of the diffusion parameter D and for a) the high flow condition in August 2019 and b) lower flow condition in September 2019.

References

Alley, R., Cuffey, K., Evenson, E., Strasser, J., Lawson, D., and Larson, G.: How glaciers entrain and transport basal sediment: Physical constraints, Quaternary Science Reviews, 16, 1017–1038, https://doi.org/10.1016/S0277-3791(97)00034-6, 1997.

Andermann, C., Longuevergne, L., Bonnet, S., Crave, A., Davy, P., and Gloaguen, R.: Impact of transient groundwater storage on the discharge of Himalayan rivers, Nature Geoscience, 5, 127–132, https://doi.org/10.1038/ngeo1356, 2012.

Anderson, M. P.: Hydrogeologic facies models to delineate large-scale spatial trends in glacial and glaciofluvial sediments, Geological Society of America Bulletin, 101, 501–511, https://doi.org/10.1130/0016-7606(1989)101<0501:HFMTDL>2.3.CO;2, 1989.

Baewert, H. and Morche, D.: Coarse sediment dynamics in a proglacial fluvial system (Fagge River, Tyrol), Geomorphology, 218, 88–97, https://doi.org/10.1016/j.geomorph.2013.10.021, 2014.

Ballantyne, C. K.: Paraglacial geomorphology, Quaternary Science Reviews, 21, 1935–2017, https://doi.org/10.1016/S0277-3791(02)00005-7, 2002.

Baraer, M., Mckenzie, J., Mark, B. G., Gordon, R., Bury, J., Condom, T., Gomez, J., Knox, S., and Fortner, S. K.: Contribution of groundwater to the outflow from ungauged glacierized catchments: A multi-site study in the tropical Cordillera Blanca, Peru, Hydrological Processes, 29, 2561–2581, https://doi.org/10.1002/hyp.10386, 2015.

Barandun, M., Huss, M., Usubaliev, R., Azisov, E., Berthier, E., Kääb, A., Bolch, T., and Hoelzle, M.: Multi-decadal mass balance series of three Kyrgyz glaciers inferred from modelling constrained with repeated snow line observations, Cryosphere, 12, 1899–1919, https://doi.org/10.5194/tc-12-1899-2018, 2018.

https://doi.org/10.5194/hess-2022-110
Preprint. Discussion started: 25 April 2022

Barnett, T. P., Adam, J. C., and Lettenmaier, D. P.: Potential impacts of a warming climate on water availability in snow-dominated regions, Nature, 438, 303–309, https://doi.org/10.1038/nature04141, 2005.

Benettin, P., Soulsby, C., Birkel, C., Tetzlaff, D., Botter, G., and Rinaldo, A.: Using SAS functions and high-resolution isotope data to unravel travel time distributions in headwater catchments, Water Resources Research, 53, 1864–1878, https://doi.org/10.1002/2016WR020117, 2017.

Beniston, M., Farinotti, D., Stoffel, M., Andreassen, L. M., Coppola, E., Eckert, N., Fantini, A., Giacona, F., Hauck, C., Huss, M., Huwald, H., Lehning, M., López-Moreno, J. I., Magnusson, J., Marty, C., Morán-Tejéda, E., Morin, S., Naaim, M., Provenzale, A., Rabatel, A., Six, D., Stötter, J., Strasser, U., Terzago, S., and Vincent, C.: The European mountain cryosphere: A review of its current state, trends, and future challenges, Cryosphere, 12, 759–794, https://doi.org/10.5194/tc-12-759-2018, 2018.

Bennett, M. R.: Glacial geology : ice sheets and landforms, Chichester : Wiley, 2nd ed.. edn., 2009.

Berghuijs, W. R., Woods, R. A., and Hrachowitz, M.: A precipitation shift from snow towards rain leads to a decrease in streamflow, Nature Climate Change, 4, 583–586, https://doi.org/10.1038/nclimate2246, 2014.

Beria, H., Larsen, J. R., Ceperley, N. C., Michelon, A., Vennemann, T., and Schaefli, B.: Understanding snow hydrological processes through the lens of stable water isotopes, Wiley Interdisciplinary Reviews: Water, 5, 1–23, https://doi.org/10.1002/wat2.1311, 2018.

Berne, A., Uijlenhoet, R., and Troch, P. A.: Similarity analysis of subsurface flow response of hillslopes with complex geometry, Water Resources Research, 41, 1–10, https://doi.org/10.1029/2004WR003629, 2005.

Berthling, I.: Beyond confusion: Rock glaciers as cryo-conditioned landforms, Geomorphology, 131, 98–106, https://doi.org/10.1016/j.geomorph.2011.05.002, 2011.

Boussinesq, J.: Recherches théoriques sur l'écoulement des nappes d'eau infiltrées dans le sol et sur le débit des sources, Journal de Mathématiques Pures et Appliquées, 10, 5–78, http://eudml.org/doc/235283, 1904.

Bovis, M. J.: Rock-slope deformation at Affliction Creek, southern Coast Mountains, British Columbia, Canadian Journal of Earth Sciences, 27, 243–254, https://doi.org/10.1139/e90-024, 1990.

Brand, G., Pohjola, V., and Hooke, R. L.: Evidence for a Till Layer Beneath Storglaciären, Sweden, Based on Electrical Resistivity Measurements, Journal of Glaciology, 33, 311–314, https://doi.org/10.1017/S0022143000008881, 1987.

Brighenti, S., Tolotti, M., Bruno, M. C., Engel, M., Wharton, G., Cerasino, L., Mair, V., and Bertoldi, W.: After the peak water: the increasing influence of rock glaciers on alpine river systems, Hydrological Processes, 33, 2804–2823, https://doi.org/10.1002/hyp.13533, 2019a.

Brighenti, S., Tolotti, M., Bruno, M. C., Wharton, G., Pusch, M. T., and Bertoldi, W.: Ecosystem shifts in Alpine streams under glacier retreat and rock glacier thaw: A review, Science of the Total Environment, 675, 542–559, https://doi.org/10.1016/j.scitotenv.2019.04.221, 2019b.

Buytaert, W., Moulds, S., Acosta, L., De Bièvre, B., Olmos, C., Villacis, M., Tovar, C., and Verbist, K. M. J.: Glacial melt content of water use in the tropical Andes, Environmental Research Letters, 12, https://doi.org/10.1088/1748-9326/aa926c, 2017.

Caballero, Y., Jomelli, V., Chevallier, P., and Ribstein, P.: Hydrological characteristics of slope deposits in high tropical mountains (Cordillera Real, Bolivia), CATENA, 47, 101–116, https://doi.org/10.1016/S0341-8162(01)00179-5, 2002.

Carrivick, J. L. and Heckmann, T.: Short-term geomorphological evolution of proglacial systems, Geomorphology, 287, 3–28, https://doi.org/10.1016/j.geomorph.2017.01.037, 2017.

Carrivick, J. L., Heckmann, T., Turner, A., and Fischer, M.: An assessment of landform composition and functioning with the first proglacial systems dataset of the central European Alps, Geomorphology, 321, 117–128, https://doi.org/10.1016/j.geomorph.2018.08.030, 2018.

https://doi.org/10.5194/hess-2022-110
Preprint. Discussion started: 25 April 2022

875 Christensen, N. S. and Lettenmaier, D. P.: A multimodel ensemble approach to assessment of climate change impacts on the hydrology and water resources of the Colorado River Basin, Hydrology and Earth System Sciences, 11, 1417–1434, https://doi.org/10.5194/hess-11-1417-2007, 2007.

Clark, M. P., Rupp, D. E., Woods, R. A., Tromp-van Meerveld, H. J., Peters, N. E., and Freer, J. E.: Consistency between hydrological models and field observations: linking processes at the hillslope scale to hydrological responses at the watershed scale, Hydrological Processes, 880 23, 311–319, https://doi.org/10.1002/hyp.7154, 2009.

Clow, D., Schrott, L., Webb, R., Campbell, D., Torizzo, A., and Dornblaser, M.: Ground Water Occurrence and Contributions to Streamflow in an Alpine Catchment, Colorado Front Range, Ground Water, 41, 937–950, https://doi.org/10.1111/j.1745-6584.2003.tb02436.x, 2003.

Cochand, M., Christe, P., Ornstein, P., and Hunkeler, D.: Groundwater Storage in High Alpine Catchments and Its Contribution to Streamflow, Water Resources Research, 55, 2613–2630, https://doi.org/10.1029/2018WR022989, 2019.

885 Crossman, J., Bradley, C., Boomer, I., and Milner, A.: Water flow dynamics of groundwater-fed streams and their ecological significance in a glacierized catchment, Arctic, Antarctic, and Alpine Research, 43, 364–379, https://doi.org/10.1657/1938-4246-43.3.364, 2011.

Curry, A. M. and Ballantyne, C. K.: Paraglacial Modification of Glacigenic Sediment, Geografiska Annaler, Series A: Physical Geography, 81, 409–419, https://doi.org/10.1111/1468-0459.00070, 1999.

Dewandel, B., Lachassagne, P., Bakalowicz, M., Weng, P., and Al-Malki, A.: Evaluation of aquifer thickness by analysing recession hy-890 drographs. Application to the Oman ophiolite hard-rock aquifer, Journal of Hydrology, 274, 248–269, https://doi.org/10.1016/S0022-1694(02)00418-3, 2003.

Dusik, J.-M., Neugirg, F., and Haas, F.: Geomorphology of Proglacial Systems, in: Geomorphology of Proglacial Systems. Geography of the Physical Environment., edited by Heckmann, T. and Morche, D., pp. 177–196, Springer, Cham, https://doi.org/10.1007/978-3-319-94184-4_11, 2019.

895 Engel, M., Penna, D., Bertoldi, G., Dell'Agnese, A., Soulsby, C., and Comiti, F.: Identifying run-off contributions during melt-induced run-off events in a glacierized alpine catchment, Hydrological Processes, 30, 343–364, https://doi.org/10.1002/hyp.10577, 2016.

Engel, M., Penna, D., Bertoldi, G., Vignoli, G., Tirler, W., and Comiti, F.: Controls on spatial and temporal variability in streamflow and hydrochemistry in a glacierized catchment, Hydrology and Earth System Sciences, 23, 2041–2063, https://doi.org/10.5194/hess-23-2041-2019, 2019.

900 Evans, D., Phillips, E., Hiemstra, J., and Auton, C.: Subglacial till: Formation, sedimentary characteristics and classification, Earth-Science Reviews, 78, 115–176, https://doi.org/10.1016/j.earscirev.2006.04.001, 2006.

Eyles, N., Eyles, C. H., and Miall, A. D.: Lithofacies types and vertical profile models; an alternative approach to the description and environmental interpretation of glacial diamict and diamictite sequences, Sedimentology, 30, 393–410, https://doi.org/10.1111/j.1365-3091.1983.tb00679.x, 1983.

905 Fayad, A., Gascoin, S., Faour, G., López-Moreno, J. I., Drapeau, L., Page, M. L., and Escadafal, R.: Snow hydrology in Mediterranean mountain regions: A review, Journal of Hydrology, 551, 374–396, https://doi.org/10.1016/j.jhydrol.2017.05.063, 2017.

Fischer, M., Huss, M., Barboux, C., and Hoelzle, M.: The New Swiss Glacier Inventory SGI2010: Relevance of Using High-Resolution Source Data in Areas Dominated by Very Small Glaciers, Arctic, Antarctic, and Alpine Research, 46, 933–945, https://doi.org/10.1657/1938-4246-46.4.933, 2014.

910 Gabbi, J., Farinotti, D., Bauder, A., and Maurer, H.: Ice volume distribution and implications on runoff projections in a glacierized catchment, Hydrology and Earth System Sciences, 16, 4543–4556, https://doi.org/10.5194/hess-16-4543-2012, 2012.

https://doi.org/10.5194/hess-2022-110
Preprint. Discussion started: 25 April 2022

Gabbi, J., Carenzo, M., Pellicciotti, F., Bauder, A., and Funk, M.: A comparison of empirical and physically based glacier surface melt models for long-term simulations of glacier response, Journal of Glaciology, 60, 1199–1207, https://doi.org/10.3189/2014JoG14J011, 2014.

Gärtner-Roer, I. and Bast, A.: (Ground) Ice in the Proglacial Zone, in: Geomorphology of Proglacial Systems. Geography of the Physical Environment., edited by Heckmann, T. and Morche, D., pp. 85–98, Springer, Cham, https://doi.org/10.1007/978-3-319-94184-4_6, 2019.

GLAMOS (1881-2020): The Swiss Glaciers 1880-2018/19, Glaciological Reports No 1-140, Yearbooks of the Cryospheric Commission of the Swiss Academy of Sciences (SCNAT), published since 1964 by VAW / ETH Zurich, https://doi.org/10.18752/glrep_series.

Glas, R., Lautz, L., McKenzie, J., Mark, B., Baraer, M., Chavez, D., and Maharaj, L.: A review of the current state of knowledge of proglacial hydrogeology in the Cordillera Blanca, Peru, WIREs Water, 5, e1299, https://doi.org/10.1002/wat2.1299, 2018.

Gordon, R. P., Lautz, L. K., McKenzie, J. M., Mark, B. G., Chavez, D., and Baraer, M.: Sources and pathways of stream generation in tropical proglacial valleys of the Cordillera Blanca, Peru, Journal of Hydrology, 522, 628–644, https://doi.org/10.1016/j.jhydrol.2015.01.013, 2015.

Grämiger, L. M., Moore, J. R., Gischig, V. S., Ivy-Ochs, S., and Loew, S.: Beyond debuttressing: Mechanics of paraglacial rock slope damage during repeat glacial cycles, Journal of Geophysical Research: Earth Surface, 122, 1004–1036, https://doi.org/10.1002/2016JF003967, 2017.

Guillon, H., Mugnier, J.-L., Buoncristiani, J.-F., Carcaillet, J., Godon, C., Prud'homme, C., van der Beek, P., and Vassallo, R.: Improved discrimination of subglacial and periglacial erosion using 10 Be concentration measurements in subglacial and supraglacial sediment load of the Bossons glacier (Mont Blanc massif, France), Earth Surface Processes and Landforms, 40, 1202–1215, https://doi.org/10.1002/esp.3713, 2015.

Haeberli, W. and Weingartner, R.: In full transition: Key impacts of vanishing mountain ice on water-security at local to global scales, Water Security, 11, 100 074, https://doi.org/10.1016/j.wasec.2020.100074, 2020.

Haeberli, W., Hallet, B., Arenson, L., Elconin, R., Humlum, O., Kääb, A., Kaufmann, V., Ladanyi, B., Matsuoka, N., Springman, S., and Mühll, D. V.: Permafrost creep and rock glacier dynamics, Permafrost and Periglacial Processes, 17, 189–214, https://doi.org/10.1002/ppp.561, 2006.

Haeberli, W., Schaub, Y., and Huggel, C.: Increasing risks related to landslides from degrading permafrost into new lakes in de-glaciating mountain ranges, Geomorphology, 293, 405–417, https://doi.org/10.1016/j.geomorph.2016.02.009, 2017.

Hallet, B., Hunter, L., and Bogen, J.: Rates of erosion and sediment evacuation by glaciers: A review of field data and their implications, Global and Planetary Change, 12, 213–235, https://doi.org/10.1016/0921-8181(95)00021-6, 1996.

Hammer, K. M. and Smith, N. D.: Sediment production and transport in a proglacial stream: Hilda Glacier, Alberta, Canada, Boreas, 12, 91–106, https://doi.org/10.1111/j.1502-3885.1983.tb00441.x, 1983.

Harbor, J.: Influence of subglacial drainage conditions on the velocity distribution within a glacier cross section, Geology, 25, 739–742, https://doi.org/10.1130/0091-7613(1997)025<0739:IOSDCO>2.3.CO;2, 1997.

Harman, C. and Sivapalan, M.: A similarity framework to assess controls on shallow subsurface flow dynamics in hillslopes, Water Resources Research, 45, 1–12, https://doi.org/10.1029/2008WR007067, 2009a.

Harman, C. and Sivapalan, M.: Effects of hydraulic conductivity variability on hillslope-scale shallow subsurface flow response and storage-discharge relations, Water Resources Research, 45, 1–15, https://doi.org/10.1029/2008WR007228, 2009b.

Harman, C. J., Sivapalan, M., and Kumar, P.: Power law catchment-scale recessions arising from heterogeneous linear small-scale dynamics, Water Resources Research, 45, 1–13, https://doi.org/10.1029/2008WR007392, 2009.

https://doi.org/10.5194/hess-2022-110
Preprint. Discussion started: 25 April 2022

Harrington, J. S., Mozil, A., Hayashi, M., and Bentley, L. R.: Groundwater flow and storage processes in an inactive rock glacier, Hydrological Processes, 32, 3070–3088, https://doi.org/10.1002/hyp.13248, 2018.

Hart, J. K.: The deforming bed/debris-rich basal ice continuum and its implications for the formation of glacial landforms (Flutes) and sediments (Melt-out till), Quaternary Science Reviews, 17, 737–754, https://doi.org/10.1016/S0277-3791(98)00065-6, 1998.

Hartmann, A., Semenova, E., Weiler, M., and Blume, T.: Field observations of soil hydrological flow path evolution over 10 millennia, Hydrology and Earth System Sciences, 24, 3271–3288, https://doi.org/10.5194/hess-24-3271-2020, 2020.

Hayashi, M.: Alpine Hydrogeology: The Critical Role of Groundwater in Sourcing the Headwaters of the World, Groundwater, 58, 498–510, https://doi.org/10.1111/gwat.12965, 2020.

He, Z., Unger-Shayesteh, K., Vorogushyn, S., Weise, S. M., Kalashnikova, O., Gafurov, A., Duethmann, D., Barandun, M., and Merz, B.: Constraining hydrological model parameters using water isotopic compositions in a glacierized basin, Central Asia, Journal of Hydrology, 571, 332–348, https://doi.org/10.1016/j.jhydrol.2019.01.048, 2019.

Heckmann, T. and Morche, D.: Geomorphology of Proglacial Systems, Geography of the Physical Environment, Springer International Publishing, Cham, https://doi.org/10.1007/978-3-319-94184-4, 2019.

Heckmann, T., Mccoll, S., and Morche, D.: Retreating ice: Research in pro-glacial areas matters, Earth Surface Processes and Landforms, 41, 271–276, https://doi.org/10.1002/esp.3858, 2016.

Heckmann, T., Morche, D., and Becht, M.: Introduction, in: Geomorphology of Proglacial Systems. Geography of the Physical Environment., edited by Heckmann, T. and Morche, D., pp. 1–19, Springer, Cham, https://doi.org/10.1007/978-3-319-94184-4_1, 2019.

Hindshaw, R. S., Tipper, E. T., Reynolds, B. C., Lemarchand, E., Wiederhold, J. G., Magnusson, J., Bernasconi, S. M., Kretzschmar, R., and Bourdon, B.: Hydrological control of stream water chemistry in a glacial catchment (Damma Glacier, Switzerland), Chemical Geology, 285, 215–230, https://doi.org/10.1016/j.chemgeo.2011.04.012, 2011.

Hogarth, W. L., Li, L., Lockington, D. A., Stagnitti, F., Parlange, M. B., Barry, D. A., Steenhuis, T. S., and Parlange, J.-Y.: Analytical approximation for the recession of a sloping aquifer, Water Resources Research, 50, 8564–8570, https://doi.org/10.1002/2014WR016084, 2014.

Hood, J. L. and Hayashi, M.: Characterization of snowmelt flux and groundwater storage in an alpine headwater basin, Journal of Hydrology, 521, 482–497, https://doi.org/10.1016/j.jhydrol.2014.12.041, 2015.

Hugentobler, M., Loew, S., Aaron, J., Roques, C., and Oestreicher, N.: Borehole monitoring of thermo-hydro-mechanical rock slope processes adjacent to an actively retreating glacier, Geomorphology, 362, 107 190, https://doi.org/10.1016/j.geomorph.2020.107190, 2020.

Huss, M. and Hock, R.: Global-scale hydrological response to future glacier mass loss, Nature Climate Change, 8, 135–140, https://doi.org/10.1038/s41558-017-0049-x, 2018.

Huss, M., Farinotti, D., Bauder, A., and Funk, M.: Modelling runoff from highly glacierized alpine drainage basins in a changing climate, Hydrological Processes, 22, 3888–3902, https://doi.org/10.1002/hyp.7055, 2008.

Huss, M., Bookhagen, B., Huggel, C., Jacobsen, D., Bradley, R. S., Clague, J. J., Vuille, M., Buytaert, W., Cayan, D. R., Greenwood, G., Mark, B. G., Milner, A. M., Weingartner, R., and Winder, M.: Toward mountains without permanent snow and ice, Earth's Future, 5, 418–435, https://doi.org/10.1002/2016EF000514, 2017.

Immerzeel, W. W., Lutz, A. F., Andrade, M., Bahl, A., Biemans, H., Bolch, T., Hyde, S., Brumby, S., Davies, B. J., Elmore, A. C., Emmer, A., Feng, M., Fernández, A., Haritashya, U., Kargel, J. S., Koppes, M., Kraaijenbrink, P. D. A., Kulkarni, A. V., Mayewski, P. A., Nepal, S., Pacheco, P., Painter, T. H., Pellicciotti, F., Rajaram, H., Rupper, S., Sinisalo, A., Shrestha, A. B., Viviroli, D., Wada, Y., Xiao, C., Yao,

T., and Baillie, J. E. M.: Importance and vulnerability of the world's water towers, Nature, 577, 364–369, https://doi.org/10.1038/s41586-019-1822-y, 2020.

Iverson, N. R., Jansson, P., and Hooke, R. L.: In-situ measurement of the strength of deforming subglacial till, Journal of Glaciology, 40, 497–503, https://doi.org/10.1017/S0022143000012375, 1994.

Jefferson, A., Nolin, A., Lewis, S., and Tague, C.: Hydrogeologic controls on streamflow sensitivity to climate variation, Hydrological Processes, 22, 4371–4385, https://doi.org/10.1002/hyp.7041, 2008.

Kalbus, E., Reinstorf, F., and Schirmer, M.: Measuring methods for groundwater - Surface water interactions: A review, Hydrology and Earth System Sciences, 10, 873–887, https://doi.org/10.5194/hess-10-873-2006, 2006.

Käser, D. and Hunkeler, D.: Contribution of alluvial groundwater to the outflow of mountainous catchments, Water Resources Research, 52, 680–697, https://doi.org/10.1002/2014WR016730, 2016.

Kaser, G., Grosshauser, M., and Marzeion, B.: Contribution potential of glaciers to water availability in different climate regimes, Proceedings of the National Academy of Sciences, 107, 20 223–20 227, https://doi.org/10.1073/pnas.1008162107, 2010.

Kirchner, J. W.: Catchments as simple dynamical systems: Catchment characterization, rainfall-runoff modeling, and doing hydrology backward, Water Resources Research, 45, https://doi.org/10.1029/2008WR006912, 2009.

Kirchner, J. W., Godsey, S. E., Solomon, M., Osterhuber, R., McConnell, J. R., and Penna, D.: The pulse of a montane ecosystem: Coupling between daily cycles in solar flux, snowmelt, transpiration, groundwater, and streamflow at Sagehen Creek and Independence Creek, Sierra Nevada, USA, Hydrology and Earth System Sciences, 24, 5095–5123, https://doi.org/10.5194/hess-24-5095-2020, 2020.

Klein, G., Vitasse, Y., Rixen, C., Marty, C., and Rebetez, M.: Shorter snow cover duration since 1970 in the Swiss Alps due to earlier snowmelt more than to later snow onset, Climatic Change, 139, 637–649, https://doi.org/10.1007/s10584-016-1806-y, 2016.

Kobierska, F., Jonas, T., Griessinger, N., Hauck, C., Huxol, S., and Bernasconi, S. M.: A multi-method field experiment to determine local groundwater flow in a glacier forefield, Hydrological Processes, 29, 817–827, https://doi.org/10.1002/hyp.10188, 2015a.

Kobierska, F., Jonas, T., Kirchner, J. W., and Bernasconi, S. M.: Linking baseflow separation and groundwater storage dynamics in an alpine basin (Dammagletscher, Switzerland), Hydrology and Earth System Sciences, 19, 3681–3693, https://doi.org/10.5194/hess-19-3681-2015, 2015b.

Kulessa, B., Hubbard, B., Williamson, M., and Brown, G. H.: Hydrogeological analysis of slug tests in glacier boreholes, Journal of Glaciology, 51, 269–280, https://doi.org/10.3189/172756505781829458, 2005.

Kurylyk, B. L. and Hayashi, M.: Inferring hydraulic properties of alpine aquifers from the propagation of diurnal snowmelt signals, Water Resources Research, 53, 4271–4285, https://doi.org/10.1002/2016WR019651, 2017.

Lane, S., Richards, K., and Chandler, J.: Discharge and sediment supply controls on erosion and deposition in a dynamic alluvial channel, Geomorphology, 15, 1–15, https://doi.org/10.1016/0169-555X(95)00113-J, 1996.

Lane, S. N. and Nienow, P. W.: Decadal-Scale Climate Forcing of Alpine Glacial Hydrological Systems, Water Resources Research, 55, 2478–2492, https://doi.org/10.1029/2018WR024206, 2019.

Lane, S. N., Bakker, M., Gabbud, C., Micheletti, N., and Saugy, J. N.: Sediment export, transient landscape response and catchment-scale connectivity following rapid climate warming and Alpine glacier recession, Geomorphology, 277, 210–227, https://doi.org/10.1016/j.geomorph.2016.02.015, 2017.

Langston, G., Bentley, L. R., Hayashi, M., McClymont, A., and Pidlisecky, A.: Internal structure and hydrological functions of an alpine proglacial moraine, Hydrological Processes, 2982, n/a–n/a, https://doi.org/10.1002/hyp.8144, 2011.

https://doi.org/10.5194/hess-2022-110
Preprint. Discussion started: 25 April 2022

Levy, A., Robinson, Z., Krause, S., Waller, R., and Weatherill, J.: Long-term variability of proglacial groundwater-fed hydrological systems in an area of glacier retreat, Skeiðarársandur, Iceland, Earth Surface Processes and Landforms, 40, 981–994, https://doi.org/10.1002/esp.3696, 2015.

Liljedahl, A. K., Gädeke, A., O'Neel, S., Gatesman, T. A., Douglas, T. A., and Liljedahl, A. K.: Glacierized headwater streams as aquifer recharge corridors, subarctic Alaska, Geophysical Research Letters, 44, 6876–6885, https://doi.org/10.1002/2017gl073834, 2017.

Liu, F., Williams, M. W., and Caine, N.: Source waters and flow paths in an alpine catchment, Colorado Front Range, United States, Water Resources Research, 40, 1–16, https://doi.org/10.1029/2004WR003076, 2004.

Lukas, S.: Processes of annual moraine formation at a temperate alpine valley glacier: Insights into glacier dynamics and climatic controls, Boreas, 41, 463–480, https://doi.org/10.1111/j.1502-3885.2011.00241.x, 2012.

Lukas, S. and Sass, O.: The formation of alpine lateral moraines inferred from sedimentology and radar reflection patterns: A case study from Gornergletscher, Switzerland, Geological Society Special Publication, 354, 77–92, https://doi.org/10.1144/SP354.5, 2011.

Lukas, S., Graf, A., Coray, S., and Schlüchter, C.: Genesis, stability and preservation potential of large lateral moraines of Alpine valley glaciers – towards a unifying theory based on Findelengletscher, Switzerland, Quaternary Science Reviews, 38, 27–48, https://doi.org/10.1016/j.quascirev.2012.01.022, 2012.

Macdonald, A. M., Black, A. R., Ó Dochartaigh, B. E., Everest, J., Darling, W. G., Flett, V., and Peach, D. W.: Using stable isotopes and continuous meltwater river monitoring to investigate the hydrology of a rapidly retreating Icelandic outlet glacier, Annals of Glaciology, 57, 151–158, https://doi.org/10.1017/aog.2016.22, 2016.

Mackay, J. D., Barrand, N. E., Hannah, D. M., Krause, S., Jackson, C. R., Everest, J., MacDonald, A. M., and Ó Dochartaigh, B.: Proglacial groundwater storage dynamics under climate change and glacier retreat, Hydrological Processes, 34, 5456–5473, https://doi.org/10.1002/hyp.13961, 2020.

Magnusson, J., Kobierska, F., Huxol, S., Hayashi, M., Jonas, T., and Kirchner, J. W.: Melt water driven stream and groundwater stage fluctuations on a glacier forefield (Dammagletscher, Switzerland), Hydrological Processes, 28, 823–836, https://doi.org/10.1002/hyp.9633, 2014.

Maier, F., van Meerveld, I., Greinwald, K., Gebauer, T., Lustenberger, F., Hartmann, A., and Musso, A.: Effects of soil and vegetation development on surface hydrological properties of moraines in the Swiss Alps, Catena, 187, 104 353, https://doi.org/10.1016/j.catena.2019.104353, 2020.

Maier, F., Meerveld, I., and Weiler, M.: Long-Term Changes in Runoff Generation Mechanisms for Two Proglacial Areas in the Swiss Alps II: Subsurface Flow, Water Resources Research, 57, 1–30, https://doi.org/10.1029/2021WR030223, 2021a.

Maier, F., van Meerveld, I., Meerveld, I., and Weiler, M.: Long-Term Changes in Runoff Generation Mechanisms for Two Proglacial Areas in the Swiss Alps I: Overland Flow, Water Resources Research, 57, 1–30, https://doi.org/10.1029/2021WR030221, 2021b.

Maisch, M., Haeberli, W., Hoelzle, M., and Wenzel, J.: Occurrence of rocky and sedimentary glacier beds in the Swiss Alps as estimated from glacier-inventory data, Annals of Glaciology, 28, 231–235, https://doi.org/10.3189/172756499781821779, 1999.

Maizels, J.: Sediments and landforms of modern proglacial terrestrial environments, in: Modern and Past Glacial Environments, 4, pp. 279–316, Elsevier, https://doi.org/10.1016/B978-075064226-2/50012-X, 2002.

Maizels, J. K.: Experiments on the Origin of Kettle-holes, Journal of Glaciology, 18, 291–303, https://doi.org/10.3189/S0022143000021365, 1977.

Malard, F., Tockner, K., and Ward, J. V.: Shifting dominance of subcatchment water sources and flow paths in a glacial floodplain, Val Roseg, Switzerland, Arctic, Antarctic, and Alpine Research, 31, 135–150, https://doi.org/10.2307/1552602, 1999.

https://doi.org/10.5194/hess-2022-110
Preprint. Discussion started: 25 April 2022

Mancini, D. and Lane, S. N.: Changes in sediment connectivity following glacial debuttressing in an Alpine valley system, Geomorphology, 352, 106 987, https://doi.org/10.1016/j.geomorph.2019.106987, 2020.

Marren, P. M.: Magnitude and frequency in proglacial rivers: A geomorphological and sedimentological perspective, Earth-Science Reviews, 70, 203–251, https://doi.org/10.1016/j.earscirev.2004.12.002, 2005.

McClymont, A. F., Roy, J. W., Hayashi, M., Bentley, L. R., Maurer, H., and Langston, G.: Investigating groundwater flow paths within proglacial moraine using multiple geophysical methods, Journal of Hydrology, 399, 57–69, https://doi.org/10.1016/j.jhydrol.2010.12.036, 2011.

McGuire, K. J. and McDonnell, J. J.: A review and evaluation of catchment transit time modeling, Journal of Hydrology, 330, 543–563, https://doi.org/10.1016/j.jhydrol.2006.04.020, 2006.

McGuire, K. J., McDonnell, J. J., Weiler, M., Kendall, C., McGlynn, B. L., Welker, J. M., and Seibert, J.: The role of topography on catchment-scale water residence time, Water Resources Research, 41, 1–14, https://doi.org/10.1029/2004WR003657, 2005.

Miall, A. D.: A review of the braided-river depositional environment, Earth Science Reviews, 13, 1–62, https://doi.org/10.1016/0012-8252(77)90055-1, 1977.

Miller, H. R. and Lane, S. N.: Biogeomorphic feedbacks and the ecosystem engineering of recently deglaciated terrain, Progress in Physical Geography, 43, 24–45, https://doi.org/10.1177/0309133318816536, 2018.

Milner, A. M., Brown, L. E., and Hannah, D. M.: Hydroecological response of river systems to shrinking glaciers, Hydrological Processes, 23, 62–77, https://doi.org/10.1002/hyp.7197, 2009.

Milner, A. M., Khamis, K., Battin, T. J., Brittain, J. E., Barrand, N. E., Füreder, L., Cauvy-Fraunié, S., Gíslason, G. M., Jacobsen, D., Hannah, D. M., Hodson, A. J., Hood, E., Lencioni, V., Ólafsson, J. S., Robinson, C. T., Tranter, M., and Brown, L. E.: Glacier shrinkage driving global changes in downstream systems, Proceedings of the National Academy of Sciences, 114, 9770–9778, https://doi.org/10.1073/pnas.1619807114, 2017.

Muir, D. L., Hayashi, M., and McClymont, A. F.: Hydrological storage and transmission characteristics of an alpine talus, Hydrological Processes, 25, n/a–n/a, https://doi.org/10.1002/hyp.8060, 2011.

Müller, T.: Weather dataset from Otemma glacier forefield, Switzerland (from 14 July 2019 to 18 November 2021) (v1.2021.02), Zenodo [Data set], https://doi.org/10.5281/zenodo.6106778, 2022a.

Müller, T.: Water table elevation and groundwater temperature from the outwash plain of the Otemma glacier forefield (Switzerland) from 2019 to 2021 (v1.2022.03), Zenodo [Data set], https://doi.org/10.5281/zenodo.6355474, 2022b.

Müller, T.: Electrical Resistivity Tomography (ERT) datasets from the Otemma glacier forefield and outwash plain (v1.2022.03), Zenodo [Data set], https://doi.org/10.5281/zenodo.6342767, 2022c.

Müller, T. and Miesen, F.: Stream discharge, stage, electrical conductivity & temperature dataset from Otemma glacier forefield, Switzerland (from July 2019 to October 2021) (v1.2021.02), Zenodo [Data set], https://doi.org/10.5281/zenodo.6202732, 2022.

Nie, Y., Liu, Q., Wang, J., Zhang, Y., Sheng, Y., and Liu, S.: An inventory of historical glacial lake outburst floods in the Himalayas based on remote sensing observations and geomorphological analysis, Geomorphology, 308, 91–106, https://doi.org/10.1016/j.geomorph.2018.02.002, 2018.

Ó Dochartaigh, B. É., MacDonald, A. M., Black, A. R., Everest, J., Wilson, P., Darling, W. G., Jones, L., and Raines, M.: Groundwater–glacier meltwater interaction in proglacial aquifers, Hydrology and Earth System Sciences, 23, 4527–4539, https://doi.org/10.5194/hess-23-4527-2019, 2019.

https://doi.org/10.5194/hess-2022-110
Preprint. Discussion started: 25 April 2022


Hydrology and Earth System Sciences
Discussions

Oestreicher, N., Loew, S., Roques, C., Aaron, J., Gualandi, A., Longuevergne, L., Limpach, P., and Hugentobler, M.: Controls on Spatial and Temporal Patterns of Slope Deformation in an Alpine Valley, Journal of Geophysical Research: Earth Surface, 126, https://doi.org/10.1029/2021JF006353, 2021.

Otto, J.-C.: Proglacial Lakes in High Mountain Environments, in: Geomorphology of Proglacial Systems. Geography of the Physical Environment., edited by Heckmann, T. and Morche, D., pp. 231–247, Springer, Cham, https://doi.org/10.1007/978-3-319-94184-4_14, 2019.

Parriaux, A. and Nicoud, G.: Hydrological behaviour of glacial deposits in mountainous areas, IAHS Publication 190, 1, 291—-312., http://infoscience.epfl.ch/record/116598, 1990.

Penna, D., Engel, M., Mao, L., Dell'agnese, A., Bertoldi, G., and Comiti, F.: Tracer-based analysis of spatial and temporal variations of water sources in a glacierized catchment, Hydrology and Earth System Sciences, 18, 5271–5288, https://doi.org/10.5194/hess-18-5271-2014, 2014.

Penna, D., Engel, M., Bertoldi, G., and Comiti, F.: Towards a tracer-based conceptualization of meltwater dynamics and streamflow response in a glacierized catchment, Hydrology and Earth System Sciences, 21, 23–41, https://doi.org/10.5194/hess-21-23-2017, 2017.

Robinson, Z. P., Fairchild, I. J., and Russell, A. J.: Hydrogeological implications of glacial landscape evolution at Skeiðarársandur, SE Iceland, Geomorphology, 97, 218–236, https://doi.org/10.1016/j.geomorph.2007.02.044, 2008.

Rogger, M., Chirico, G. B., Hausmann, H., Krainer, K., Brückl, E., Stadler, P., and Blöschl, G.: Impact of mountain permafrost on flow path and runoff response in a high alpine catchment, Water Resources Research, 53, 1288–1308, https://doi.org/10.1002/2016WR019341, 2017.

Roncoroni, M., Brandani, J., Battin, T. I., and Lane, S. N.: Ecosystem engineers: Biofilms and the ontogeny of glacier floodplain ecosystems, Wiley Interdisciplinary Reviews: Water, 6, e1390, https://doi.org/10.1002/wat2.1390, 2019.

Rupp, D. E. and Selker, J. S.: Drainage of a horizontal Boussinesq aquifer with a power law hydraulic conductivity profile, Water Resources Research, 41, 1–8, https://doi.org/10.1029/2005WR004241, 2005.

Rupp, D. E. and Selker, J. S.: On the use of the Boussinesq equation for interpreting recession hydrographs from sloping aquifers, Water Resources Research, 42, 1–15, https://doi.org/10.1029/2006WR005080, 2006.

Santos, A. C., Portela, M. M., Rinaldo, A., and Schaefli, B.: Analytical flow duration curves for summer streamflow in Switzerland, Hydrology and Earth System Sciences, 22, 2377–2389, https://doi.org/10.5194/hess-22-2377-2018, 2018.

Sass, O.: Determination of the internal structure of alpine talus deposits using different geophysical methods (Lechtaler Alps, Austria), Geomorphology, 80, 45–58, https://doi.org/10.1016/j.geomorph.2005.09.006, 2006.

Sass, O.: Bedrock detection and talus thickness assessment in the European Alps using geophysical methods, Journal of Applied Geophysics, 62, 254–269, https://doi.org/10.1016/j.jappgeo.2006.12.003, 2007.

Schaefli, B., Nicótina, L., Imfeld, C., Da Ronco, P., Bertuzzo, E., and Rinaldo, A.: SEHR-ECHO v1.0: A spatially explicit hydrologic response model for ecohydrologic applications, Geoscientific Model Development, 7, 2733–2746, https://doi.org/10.5194/gmd-7-2733-2014, 2014.

Schilling, O. S., Parajuli, A., Tremblay Otis, C., Müller, T. U., Antolinez Quijano, W., Tremblay, Y., Brennwald, M. S., Nadeau, D. F., Jutras, S., Kipfer, R., and Therrien, R.: Quantifying Groundwater Recharge Dynamics and Unsaturated Zone Processes in Snow-Dominated Catchments via On-Site Dissolved Gas Analysis, Water Resources Research, 57, 1–24, https://doi.org/10.1029/2020WR028479, 2021.

Schmieder, J., Garvelmann, J., Marke, T., and Strasser, U.: Spatio-temporal tracer variability in the glacier melt end-member - How does it affect hydrograph separation results?, Hydrological Processes, 32, 1828–1843, https://doi.org/10.1002/hyp.11628, 2018.

Schmieder, J., Seeger, S., Weiler, M., and Strasser, U.: 'Teflon Basin' or Not? A High-Elevation Catchment Transit Time Modeling Approach, Hydrology, 6, 92, https://doi.org/10.3390/hydrology6040092, 2019.

https://doi.org/10.5194/hess-2022-110
Preprint. Discussion started: 25 April 2022

Somers, L. D., Gordon, R. P., McKenzie, J. M., Lautz, L. K., Wigmore, O., Glose, A. M., Glas, R., Aubry-Wake, C., Mark, B., Baraer, M., and Condom, T.: Quantifying groundwater–surface water interactions in a proglacial valley, Cordillera Blanca, Peru, Hydrological Processes, 30, 2915–2929, https://doi.org/10.1002/hyp.10912, 2016.

Staudinger, M., Stoelzle, M., Seeger, S., Seibert, J., Weiler, M., and Stahl, K.: Catchment water storage variation with elevation, Hydrological Processes, 31, 2000–2015, https://doi.org/10.1002/hyp.11158, 2017.

Stewart, M. K.: Promising new baseflow separation and recession analysis methods applied to streamflow at Glendhu Catchment, New Zealand, Hydrology and Earth System Sciences, 19, 2587–2603, https://doi.org/10.5194/hess-19-2587-2015, 2015.

Swift, D. A., Nienow, P. W., Hoey, T. B., and Mair, D. W. F.: Seasonal evolution of runoff from Haut Glacier d'Arolla, Switzerland and implications for glacial geomorphic processes, Journal of Hydrology, 309, 133–148, https://doi.org/10.1016/j.jhydrol.2004.11.016, 2005.

Temme, A. J. A. M.: The Uncalm Development of Proglacial Soils in the European Alps Since 1850, pp. 315–326, Springer, Cham, https://doi.org/10.1007/978-3-319-94184-4_18, 2019.

Troch, P. A., Berne, A., Bogaart, P., Harman, C., Hilberts, A. G., Lyon, S. W., Paniconi, C., Pauwels, V. R., Rupp, D. E., Selker, J. S., Teuling, A. J., Uijlenhoet, R., and Verhoest, N. E.: The importance of hydraulic groundwater theory in catchment hydrology: The legacy of Wilfried Brutsaert and Jean-Yves Parlange, Water Resources Research, 49, 5099–5116, https://doi.org/10.1002/wrcr.20407, 2013.

Tromp-Van Meerveld, H. J. and McDonnell, J. J.: Threshold relations in subsurface stormflow: 2. The fill and spill hypothesis, Water Resources Research, 42, 1–11, https://doi.org/10.1029/2004WR003800, 2006.

Van Tiel, M., Kohn, I., Van Loon, A. F., and Stahl, K.: The compensating effect of glaciers: Characterizing the relation between interannual streamflow variability and glacier cover, Hydrological Processes, 34, 553–568, https://doi.org/10.1002/hyp.13603, 2020.

Van Tiel, M., Van Loon, A. F., Seibert, J., and Stahl, K.: Hydrological response to warm and dry weather: do glaciers compensate?, Hydrology and Earth System Sciences, 25, 3245–3265, https://doi.org/10.5194/hess-25-3245-2021, 2021.

Verhoest, N. E. C. and Troch, P. A.: Some analytical solutions of the linearized Boussinesq equation with recharge for a sloping aquifer, Water Resources Research, 36, 793–800, https://doi.org/10.1029/1999WR900317, 2000.

Vincent, A., Violette, S., and Aðalgeirsdóttir, G.: Groundwater in catchments headed by temperate glaciers: A review, Earth-Science Reviews, 188, 59–76, https://doi.org/10.1016/j.earscirev.2018.10.017, 2019.

Viviroli, D., Dürr, H. H., Messerli, B., Meybeck, M., and Weingartner, R.: Mountains of the world, water towers for humanity: Typology, mapping, and global significance, Water Resources Research, 43, 1–13, https://doi.org/10.1029/2006WR005653, 2007.

Viviroli, D., Kummu, M., Meybeck, M., and Wada, Y.: Increasing dependence of lowland population on mountain water resources, EartArXiv, https://doi.org/10.31223/osf.io/fr5uj, 2019.

Vuille, M., Carey, M., Huggel, C., Buytaert, W., Rabatel, A., Jacobsen, D., Soruco, A., Villacis, M., Yarleque, C., Elison Timm, O., Condom, T., Salzmann, N., and Sicart, J. E.: Rapid decline of snow and ice in the tropical Andes – Impacts, uncertainties and challenges ahead, Earth-Science Reviews, 176, 195–213, https://doi.org/10.1016/j.earscirev.2017.09.019, 2018.

Wagener, T., Sivapalan, M., Troch, P., and Woods, R.: Catchment Classification and Hydrologic Similarity, Geography Compass, 1, 901–931, https://doi.org/10.1111/j.1749-8198.2007.00039.x, 2007.

Ward, J. V., Malard, F., Tockner, K., and Uehlinger, U.: Influence of ground water on surface water conditions in a glacial flood plain of the Swiss Alps, Hydrological Processes, 13, 277–293, https://doi.org/10.1002/(SICI)1099-1085(19990228)13:3<277::AID-HYP738>3.0.CO;2-N, 1999.

Werder, M. A., Hewitt, I. J., Schoof, C. G., and Flowers, G. E.: Modeling channelized and distributed subglacial drainage in two dimensions, Journal of Geophysical Research: Earth Surface, 118, 2140–2158, https://doi.org/10.1002/jgrf.20146, 2013.

https://doi.org/10.5194/hess-2022-110
Preprint. Discussion started: 25 April 2022

Williams, M. W., Hood, E., Molotch, N. P., Caine, N., Cowie, R., and Liu, F.: The 'teflon basin' myth: hydrology and hydrochemistry of a seasonally snow-covered catchment, Plant Ecology & Diversity, 8, 639–661, https://doi.org/10.1080/17550874.2015.1123318, 2015.

Winkler, G., Wagner, T., Pauritsch, M., Birk, S., Kellerer-Pirklbauer, A., Benischke, R., Leis, A., Morawetz, R., Schreilechner, M. G., and Hergarten, S.: Identification and assessment of groundwater flow and storage components of the relict Schöneben Rock Glacier, Niedere Tauern Range, Eastern Alps (Austria), Hydrogeology Journal, 24, 937–953, https://doi.org/10.1007/s10040-015-1348-9, 2016.

Wittenberg, H. and Sivapalan, M.: Watershed groundwater balance estimation using streamflow recession analysis and baseflow separation, Journal of Hydrology, 219, 20–33, https://doi.org/10.1016/S0022-1694(99)00040-2, 1999.

Yao, Y., Zheng, C., Andrews, C. B., Scanlon, B. R., Kuang, X., Zeng, Z., Jeong, S. J., Lancia, M., Wu, Y., and Li, G.: Role of Groundwater in Sustaining Northern Himalayan Rivers, Geophysical Research Letters, 48, 1–10, https://doi.org/10.1029/2020GL092354, 2021.

Zielinski, T. and Van Loon, A.: Pleistocene sandur deposits represent braidplains, not alluvial fans, Boreas, 32, 590–611, https://doi.org/10.1080/03009480310004170, 2003.

Zuecco, G., Carturan, L., De Blasi, F., Seppi, R., Zanoner, T., Penna, D., Borga, M., Carton, A., and Dalla Fontana, G.: Understanding hydrological processes in glacierized catchments: Evidence and implications of highly variable isotopic and electrical conductivity data, Hydrological Processes, 33, 816–832, https://doi.org/10.1002/hyp.13366, 2019.